vimentin mouse monoclonal antibody (1:200; Dako Cytomation, Copenhagen, Denmark), anti-fibronectin mouse monoclonal antibody (1:400; Chemicon International, Temecula, CA), anti-nestin rabbit polyclonal antibody (1:400; Chemicon International), and anti-CD44 mouse monoclonal antibody (1:400; Serotec Ltd., Oxford, England). Cell nuclei were stained with DAPI (1:1000, Molecular Probes). We omitted the primary antibodies for negative controls. After reacting with primary antibodies, sections were incubated with appropriate secondary antibodies.

4.2. *Animal surgery*

For experimental spinal cord injury (SCI), we used a total of 37 female Sprague–Dawley rats aged 8–10 weeks (weight 174–236 g; SLC). Fig. 7 shows the time line of the present study. Rats were anesthetized with 1.6% halothane in 0.5 L/min oxygen. Laminectomy was performed at the T9–T10 levels, and contusion injury was introduced using the Infinite Horizon impactor (IH impactor, 200 Kdyn, Precision Systems and Instrumentation, Lexington, NY). Immediately after SCI, a thin silicone tube was inserted into the subarachnoid space at the laminectomized L1 level using a surgical microscope. The tube was connected to an Alzet osmotic mini pump (model 2004; Alza, Paolo Alto, CA) containing 30 μg/μL fasudil (Asahi Kasei Inc., Tokyo, Japan) in saline. The infusion rate was 6.0 μL/day resulting in the infusion of 180 μg/day of fasudil. The infusion was continued for 4 weeks, resulting in a total fasudil infusion of approximately 5.04 mg /animal. Rats were group-housed in the animal facility and maintained under constant temperature and humidity conditions. Food and water were provided *ad libitum*. Manual bladder expression was performed twice a day until recovery of the bladder reflex. All animals were given antibiotics (500 μL/day; Bactramin, Chuugai Pharmaceutical, Tokyo, Japan) by subcutaneous administration once a day for 3 days.

Fourteen days after injury, the injured site was re-exposed and the same volume of BMSCs or saline was injected by micro-glass pipette needle attached to a 10 μL Hamilton syringe (Hamilton Company, Reno, NV). The injection was made at several depths during drawback in each injection, and the needle was left in the spinal cord for one additional minute following injection in order to minimize reflux. The injection sites were located at 4 mm intervals on the rostral and caudal edges of the lesion site (5.0×10^5 cells/μL, 2. 5 μL each, 2.5×10^6 cells/total). All animals, including control groups, were immunosuppressed with cyclosporine A (Sandimmun, Novartis, Basel, Switzerland) for the remaining experimental period (20 mg/kg on Monday and Wednesday, 40 mg/kg on Friday) (Wennersten et al., 2004). None of the animals showed abnormal behavior. All the experimental procedures were performed in compliance with the guidelines established by the Animal Care and Use Committee of Chiba University.

4.3. *Experimental groups*

The rats were randomly divided into four groups (Table 1). The fasudil+BMSC group ($n=10$) received fasudil by Alzet osmotic mini pump, as explained above and BMSCs were transplanted into the spinal cord. The fasudil-only group ($n=8$) received fasudil by Alzet pump and saline injection into the spinal cord. The BMSC-only group ($n=9$) received saline by Alzet pump and BMSC transplantation into the spinal cord. The control group ($n=10$) received saline via Alzet pump and saline injection into the spinal cord. One animal of BMSC-only group was sacrificed to make sure that BMSC was survived three weeks after BMSCs transplantation.

4.4. *Assessments of sensory motor functions*

4.4.1. *BBB open field locomotor test*

Hind limb function was assessed in an open field (100×60 cm plastic pool) using the BBB open field locomotor test (Basso et al., 1995). Measurements were performed 3 days after contusion injury and weekly thereafter for 9 weeks. Tests were videotaped and scored by two trained observers who were unaware of the treatment group.

4.4.2. *Sensory tests*

Thermal nociceptive thresholds in rat hind limbs were evaluated using a Hargreaves device (Ugo Basile, Varese, Italy). The rat was deposited into individual transparent acrylic boxes with the floor maintained at 28 °C. A heat stimulus (150 mcal/s/cm^2) was delivered using a 0.5 cm diameter radiant heat source positioned under the plantar surface of the hind limb. The heat source was placed alternately under each hind limb to avoid anticipation by the animal. A cutoff time of 22 s was used, as it had been ascertained that no tissue damage would result within this

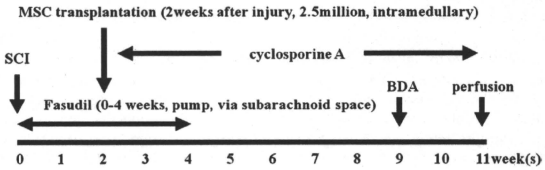

Fig. 7 – Experimental protocol. Immediately after SCI (T9–T10 levels; IH impactor, 200 Kdyn), fasudil was administered by an Alzet mini-osmotic pump via the subarachnoid space into the injury site for four weeks. Two weeks after contusion, 2.5×10^6 GFP-tagged BMSCs were transplanted into the lesion site. All animals were immunosuppressed with cyclosporin A for the remaining experimental period. BDA was injected into the sensory-motor cortex 9 weeks after contusion. Animals were perfused transcardially, and histological examination was performed eleven weeks after contusion.

Table 1 - Experimental groups.

Groups	Number of rats	Treatment	
		Infusion by Alzet pump	Transplantation
Fasudil+BMSC group	10	Fasudil	BMSC
Fasudil-only group	8	Fasudil	Saline
BMSC-only group	9	Saline	BMSC
Control group	10	Saline	Saline

The rats were randomly divided into four groups. The fasudil +BMSC group ($n=10$) received fasudil administration by Alzet osmotic mini pump and BMSC transplantation into the spinal cord. The fasudil-only group ($n=8$) received fasudil administration by Alzet pump and saline injection into the spinal cord. The BMSC-only group ($n=9$) received saline administration by Alzet pump and BMSC transplantation into the spinal cord. The control group ($n=10$) received saline administration by Alzet pump and saline injection into the spinal cord.

time period. The withdrawal threshold was calculated as the average of six consecutive tests.

Mechanical withdrawal thresholds in rat hind limbs were tested using a Dynamic Plantar Aesthesiometer (Ugo Basile), in which a mechanical stimulus was applied via an actuator filament (0.5 mm diameter), which under computer control applies a linear ramp 5.0 g/s to the plantar surface of the hind limb. The withdrawal threshold was calculated as the average of six consecutive tests. Both tests were performed 8 weeks after contusion. For comparison with baseline, we also performed both tests with normal rats ($n=31$).

4.5. *Anterograde labeling of corticospinal tracts with BDA, immunohistochemical, and histological assessment*

Nine weeks after contusion, the corticospinal tract (CST) was hemilaterally traced under halothane anesthesia with 2.0 μL biotinylated dextran amine (BDA, molecular weight: 10,000, 10% in 0.01 M PBS, Molecular Probes). A micro-glass pipette needle attached to a 2 μL Hamilton syringe was stereotaxically guided, and BDA was slowly injected into four sites in the sensorimotor cortex for the hind limb at a depth of 1 mm. The needle was left for an additional 1 min following each injection to minimize reflux.

Animals were subjected to trans-cardiac perfusion with 4% paraformaldehyde in PBS (pH 7.4) for 14 days after BDA injection. At the conclusion of the BDA infusion period (11 weeks after contusion), the spinal cords were dissected and immersed overnight in 4% paraformaldehyde, then stored in 20% sucrose in PBS. The spinal cords were cut into 20 mm lengths (10 mm rostral and 10 mm caudal from the lesion site) and embedded in OCT compound (Tissue Tek, Sakura Finetechnical, Tokyo, Japan). These blocks were sectioned in the sagittal plane (section thickness=25 μm) using a cryostat. We mounted a set of serial sections on a total of eight poly-L-lysine-coated slides (Matsunami, Tokyo, Japan) for each animal. Each slide contained six sliced sections at 200 μm intervals, and the sections for each slide were offset by 25 μm from the previous slide in the set. By this method, we were able to cover approximately 1200 μm of the lesion at 25 μm intervals in these eight slides. We processed the slides for histological or immunohistochemical staining.

To evaluate lesion size, one slide from one animal was stained with cresyl violet. The three slices showing the greatest damage were selected from one slide, and cavity size was determined with Photoshop 5.5 software (Adobe, San Jose, CA). Mean lesion size values for each group were calculated using these three lesions size values for each animal, and mean size comparisons were performed among the four groups.

In order to identify cell populations and characterize the cellular response, sections were immunolabeled with one or more antibodies. Anti-green fluorescent protein (GFP, rabbit polyclonal antibody, 1: 1600, Molecular Probes) was used to identify grafted rat BMSCs. The number of surviving transplanted cells and the localization of the cells were evaluated. Double immunohistochemical staining was performed with GFP plus either mouse anti-glial fibrillary acidic protein (GFAP, 1:400, Sigma, St. Louis, MO) or mouse anti-GSTπ (1:400, BD Pharmingen, Franklin Lakes, NJ), or mouse anti-NeuN (1:400; Chemicon) to evaluate transdifferentiation of BMSCs into astrocytes, oligodendrocytes, and neurons, respectively. After reacting with primary antibodies, the sections were incubated with Alexa Fluor 488-conjugated anti-mouse or anti-rabbit IgG (Molecular Probes) and with Alexa Fluor 594-conjugated anti-mouse or anti-rabbit IgG (Molecular Probes).

To evaluate residual and regenerative fibers, rabbit anti-neurofilament polyclonal antibody (1:800, Sigma) and rabbit anti-serotonin (5-HydroxyTryptamine, 5-HT) polyclonal antibody (1:5000, Sigma) were used for pan-nerve fibers. After reacting with primary antibodies, the sections were incubated with Alexa Fluor 488-conjugated anti-rabbit IgG (Molecular Probes) to detect positive signals. The numbers of immunoreactive fibers that traversed the virtual lines perpendicular to the central axis of the grafts were counted at three locations: the lesion site, 2.5 mm rostral from the lesion site, and 2.5 mm caudal from the lesion site.

For anterograde labeling of CSTs with BDA, sections were incubated with Alexa Fluor 594-conjugated streptavidin (1:800; Molecular Probes). The distance from the end of the labeled axons to the edge of the lesion site and the number of CST axons at the lesion site were measured.

The fluorescent signals were observed by fluorescence microscopy, ECLIPSE E600 (Nikon, Tokyo, Japan), and DP71 (Olympus, Tokyo, Japan). To maintain blinding in this histological study, observers were kept unaware of treatment groups.

4.6. *Statistical analysis*

Data were evaluated by multiple comparisons between groups. For histological studies, one-way ANOVA followed by the Bonferroni/Dunn *post hoc* test was used. For the 9-week locomotor scale, repeated-measures ANOVA followed by the Turkey-Kramer *post hoc* test was used. For fractional BBB score at each time point, one-way ANOVA followed by the Turkey-Kramer *post hoc* test was used. Data are presented as mean values ± SEM. Differences were considered statistically significant at $^{*}p<0.05$.

Acknowledgments

Fasudil was kindly provided by Asahi Kasei Corporation (Tokyo, Japan). This research was supported by grant-in-aid for Japanese scientific research grant 19591715.

REFERENCES

Ackery, A., Robins, S., Fehlings, M.G., 2006. Inhibition of Fas-mediated apoptosis through administration of soluble Fas receptor improves functional outcome and reduces posttraumatic axonal degeneration after acute spinal cord injury. J. Neurotrauma 23, 604–616.

Akiyama, Y., Radtke, C., Kocsis, J.D., 2002. Remyelination of the rat spinal cord by transplantation of identified bone marrow stromal cells. J. Neurosci. 22, 6623–6630.

Alvarez-Dolado, M., Pardal, R., Garcia-Verdugo, J.M., Fike, J.R., Lee, H.O., Pfeffer, K., Lois, C., Morrison, S.J., Alvarez-Buylla, A., 2003. Fusion of bone-marrow-derived cells with Purkinje neurons, cardiomyocytes and hepatocytes. Nature 425, 968–973.

Amano, M., Fukata, Y., Kaibuchi, K., 2000. Regulation and functions of Rho associated kinase. Exp. Cell Res. 261, 44–51.

Azizi, S.A., Stokes, D., Augelli, B.J., DiGirolamo, C., Prockop, D.J., 1998. Engraftment and migration of human bone marrow stromal cells implanted in the brains of albino rats- Similarities to astrocyte grafts. Proc. Natl. Acad. Sci. U. S. A. 95, 3908–3913.

Baptiste, D.C., Fehlings, M.G., 2006. Pharmacological approaches to repair the injured spinal cord. J. Neurotrauma 23, 318–334.

Basso, D.M., Beattie, M.S., Bresnahan, J.C., 1995. A sensitive and reliable locomotor rating scale for open field testing in rats. J. Neurotrauma 12, 1–21.

Chan, C.C., Wong, A.K., Liu, J., Steeves, J.D., Tetzlaff, W., 2007. ROCK inhibition with Y27632 activates astrocytes and increases their expression of neurite growth-inhibitory chondroitin sulfate proteoglycans. Glia 55, 369–384.

Chen, Q., Long, Y., Yuan, X., Zou, L., Sun, J., Chen, S., Perez-Polo, J.R., Yang, K., 2005. Protective effects of bone marrow stromal cell transplantation in injured rodent brain: synthesis of neurotrophic factors. J. Neurosci. Res. 80, 611–619.

Chopp, M., Zhang, X.H., Li, Y., Wang, L., Chen, J., Lu, D., Lu, M., Rosenblum, M., 2000. Spinal cord injury in rat: treatment with bone marrow stromal cell transplantation. Neuroreport 11, 3001–3005.

Chopp, M., Li, Y., 2002. Treatment of neural injury with marrow stromal cells. Lancet Neurol. 1, 92–100 Review.

Deng, W., Obrocka, M., Fischer, I., Prockop, D.J., 2001. In vitro differentiation of human stromal cells into early progenitors of neural cells by conditions that increase intracellular cyclic AMP. Biol. Biophys. Res. Commun. 282, 148–152.

Dezawa, M., Kanno, H., Hoshino, M., Cho, H., Matsumoto, N., Itokazu, Y., Tajima, N., Yamada, H., Sawada, H., Ishikawa, H., Mimura, T., Kitada, M., Suzuki, Y., Ide, C., 2004. Specific induction of neuronal cells from bone marrow stromal cells and application for autologous transplantation. J. Clin. Invest. 113, 1701–1710.

Dickson, B.J., 2001. Rho GTPases in growth cone guidance. Curr. Opin. Neurobiol. 11, 103–110.

Dubreuil, C.I., Winton, M.J., McKerracher, L., 2003. Rho activation patterns after spinal cord injury and the role of activated Rho in apoptosis in the central nervous system. J. Cell Biol. 162, 233–243.

Hara, M., Takayasu, M., Watanabe, K., Noda, A., Takagi, T., Suzuki, Y., Yoshida, J., 2000. Protein kinase inhibition by fasudil hydrochloride promotes neurological recovery after spinal cord injury in rats. J. Neurosurg. 93 (1 Suppl.), 94–101.

He, Y, Xu, H, Liang, L, Zhan, Z, Yang, X, Yu, X, Ye, Y, Sun, L., 2008. Antiinflammatory effect of Rho kinase blockade via inhibition of NF-kappaB activation in rheumatoid arthritis. Arthritis Rheum. 58, 3366–3376.

Hess, D.C., Abe, T., Hill, W.D., Studdard, A.M., Carothers, J., Masuya, M., Fleming, P.A., Drake, C.J., Ogawa, M., 2004. Hematopoietic origin of microglial and preivascular cells in brain. Exp. Neurol. 186, 134–144.

Himes, B.T., Neuhuber, B., Coleman, C., Kushner, R., Swanger, S.A., Kopen, G.C., Wagner, J., Shumsky, J.S., Fischer, I., 2006. Recovery of function following grafting of human bone marrow-derived stromal cells into the injured spinal cord. Neurorehabilitation Neural. Repair 20, 278–296.

Hofstetter, C.P., Schwarz, E.J., Hess, D., Widenfalk, J., El Manira, A., Prockop, D.J., Olson, L., 2002. Marrow stromal cells from guiding strands in the injured spinal cord and promote recovery. Proc. Natl. Acad. Sci. U. S. A. 99, 2199–2204.

Isele, N.B., Lee, H.S., Landshamer, S., Straube, A., Padovan, C.S., Plesnila, N., Culmsee, C., 2007. Bone marrow stromal cells mediate protection through stimulation of PI3-K/Akt and MAPK signaling in neurons. Neurochem. Int. 50, 243–250.

Kamada, T., Koda, M., Dezawa, M., Yoshinaga, K., Hashimoto, M., Koshizuka, S., Nishio, Y., Moriya, H., Yamazaki, M., 2005. Transplantation of bone marrow stromal cell-derived Schwann cells promotes axonal regeneration and functional recovery after complete transection of adult rat spinal cord. J. Neuropathol. Exp. Neurol. 64, 37–45.

Kim, B.J., Seo, J.H., Bubien, J.K., Oh, Y.S., 2002. Differentiation of adult bone marrow stem cells into neuroprogenitor cells in vitro. Neuroreport 13, 1185–1188.

Koda, M., Okada, S., Nakayama, T., Koshizuka, S., Kamada, T., Nishio, Y., Someya, Y., Yoshinaga, K., Okawa, A., Moriya, H., Yamazaki, M., 2005. Hematopoietic stem cell and marrow stromal cell for spinal cord injury in mice. Neuroreport 16, 1763–1767.

Kopen, G.C., Prockop, D.J., Phinney, D.G., 1999. Marrow stromal cells migrate throughout forebrain and cerebellum, and they differentiate into astrocytes after injection into neonatal mouse brains. Proc. Natl. Acad. Sci. U. S. A. 96, 10711–10716.

Koshizuka, S., Okada, S., Okawa, A., Koda, M., Murasawa, M., Hashimoto, M., Kamada, T., Yoshinaga, K., Murakami, M., Moriya, H., Yamazaki, M., 2004. Transplanted hematopoietic stem cells from bone marrow differentiate into neural lineage cells and promote functional recovery after spinal cord injury in mice. J. Neuropathol. Exp. Neurol. 63, 64–72.

Kubo, T., Yamashita, T., 2007. Rho-ROCK inhibitors for the treatment of CNS injury. Recent Patents CNS Drug Discov. 2, 173–179.

Lee, J.B., Kuroda, S., Shichinohe, H., Yano, S., Kobayashi, H., Hida, K., Iwasaki, Y., 2004. A pre-clinical assessment model of rat autogeneic bone marrow stromal cell transplantation into the central nervous system. Brain Res. Brain Res. Protoc. 14, 37–44.

Liu, X.Z., Xu, X.M., Hu, R., Du, C., Zhang, S.X., McDonald, J.W., Dong, H.X., Wu, Y.J., Fan, G.S., Jacquin, M.F., Hsu, C.Y., Choi, D.W., 1997. Neuronal and glial apoptosis after traumatic spinal cord injury. J. Neurosci. 17, 5395–5406.

Lu, P., Jones, L.L., Tuszynski, M.H., 2005. BDNF-expressing marrow stromal cells support extensive axonal growth at sites of spinal cord injury. Exp. Neurol. 191, 344–360.

Monnier, P.P., Sierra, A., Schwab, J.M., Henke-Fahle, S., Mueller, B.K., 2003. The Rho/ROCK pathway mediates neurite growth-inhibitory activity associated with the chondroitin sulfate proteoglycans of the CNS glial scar. Mol. Cell. Neurosci. 22, 319–330.

Mueller, B.K., Mack, H., Teusch, N., 2005. Rho kinase, a promising drug target for neurological disorders. Nat. Rev. Drug Discov. 4, 387–398.

Neuhuber, B., Timothy Himes, B., Shumsky, J.S., Gallo, G., Fischer, I., 2005. Axon growth and recovery of function supported by

human bone marrow stromal cells in the injured spinal cord exhibit donor variations. Brain Res. 1035, 73–85.

Nishio, Y., Koda, M., Kamada, T., Someya, Y., Kadota, R., Mannoji, C., Miyashita, T., Okada, S., Okawa, A., Moriya, H., Yamazaki, M., 2007. Granulocyte colony-stimulating factor attenuates neuronal death and promotes functional recovery after spinal cord injury in mice. J. Neuropathol. Exp. Neurol. 66, 724–731.

Ohta, M., Suzuki, Y., Noda, T., Ejiri, Y., Dezawa, M., Kataoka, K., Chou, H., Ishikawa, N., Matsumoto, N., Iwashita, Y., Mizuta, E., Kuno, S., Ide, C., 2004. Bone marrow stromal cells infused into the cerebrospinal fluid promote functional recovery of the injured rat spinal cord with reduced cavity formation. Exp. Neurol. 187, 266–278.

Ramer, LM, Borisoff, JF, Ramer, MS., 2004. Rho-kinase inhibition enhances axonal plasticity and attenuates cold hyperalgesia after dorsal rhizotomy. J Neurosci. 24, 10796–10805.

Rossignol, S., Schwab, M., Schwartz, M., Fehlings, M.G., 2007. Spinal cord injury: time to move? J. Neurosci. 27, 11782–11792 Review.

Sanchez-Ramos, J., Song, S., Cardozo-Pelaez, F., Hazzi, C., Stedeford, T., Willing, A., Freeman, T.B., Saporta, S., Janssen, W., Patel, N., Cooper, D.R., Sanberg, P.R., 2000. Adult bone marrow stromal cells differentiate into neural cells in vitro. Exp. Neurol. 164, 247–256.

Satoh, S., Toshima, Y., Ikegaki, I., Iwasaki, M., Asano, T., 2007. Wide therapeutic time window for fasudil neuroprotection against ischemia-induced delayed neuronal death in gerbils. Brain Res. 1128, 175–180.

Sauerzweig, S., Munsch, T., Lessmann, V., Reymann, K.G., Braun, H., 2009. A population of serum deprivation-induced bone marrow stem cells (SD-BMSC) expresses marker typical for embryonic and neural stem cells. Exp. Cell Res. 315, 50–66.

Shiokawa, M, Yamaguchi, T, Narita, M, Okutsu, D, Nagumo, Y, Miyoshi, K, Suzuki, M, Inoue, T, Suzuki, T., 2007. Effects of fasudil on neuropathic pain-like state in mice. Nihon Shinkei Seishin Yakurigaku Zasshi 27, 153–159 Japanese.

Someya, Y., Koda, M., Dezawa, M., Kadota, T., Hashimoto, M., Kamada, T., Nishio, Y., Kadota, R., Mannoji, C., Miyashita, T., Okawa, A., Yoshinaga, K., Yamazaki, M., 2008. Reduction of cystic cavity, promotion of axonal regeneration and sparing, and functional recovery with transplanted bone marrow stromal cell-derived Schwann cells after contusion injury to the adult rat spinal cord. J. Neurosurg. Spine 9, 600–610.

Song, S., Kamath, S., Mosquera, D., Zigova, T., Sanberg, P., Vesely, D.L., Sanchez-Ramos, J., 2004. Expression of brain natriuretic peptide by human bone marrow stromal cells. Exp. Neurol. 185, 191–197.

Sung, J.K., Miao, L., Calvert, J.W., Huang, L., Louis Harkey, H., Zhang, J.H., 2003. A possible role of RhoA/Rho-kinase in experimental spinal cord injury in rat. Brain Res. 959, 29–38.

Terada, N., Hamazaki, T., Oka, M., Hoki, M., Mastalerz, D.M., Nakano, Y., Meyer, E.M., Morel, L., Petersen, B.E., Scott, E.W., 2002. Bone marrow cells adopt the phenotype of other cells by spontaneous cell fusion. Nature 416, 542–545.

Wennersten, A., Meier, X., Holmin, S., Wahlberg, L., Mathiesen, T., 2004. Proliferation, migration, and differentiation of human neural stem/progenitor cells after transplantation into a rat model of traumatic brain injury. J. Neurosurg. 100, 88–96.

Woodbury, D., Schwarz, E.J., Prockop, D.J., Black, I.B., 2000. Adult rat and human bone marrow stromal cells differentiate into neurons. J. Neurosci. Res. 15, 364–370.

Woodbury, D., Reynolds, K., Black, I.B., 2002. Adult bone marrow stromal stem cells express germline, ectodermal, endodermal, and mesodermal genes prior to neurogenesis. J. Neurosci. Res. 69, 908–917.

Wright, K.T., El Masri, W., Osman, A., Roberts, S., Chamberlain, G., Ashton, B.A., Johnson, W.E., 2007. Bone marrow stromal cells stimulate neurite outgrowth over neural proteoglycans (CSPG), myelin associated glycoprotein and Nogo-A. Biochem. Biophys. Res. Commun. 354, 559–566.

Wu, S., Suzuki, Y., Ejiri, Y., Noda, T., Bai, H., Kitada, M., Kataoka, K., Ohta, M., Chou, H., Ide, C., 2003. Bone marrow stromal cells enhance differentiation of cocultured neurosphere cells and promote regeneration of injured spinal cord. J. Neurosci. Res. 72, 343–351.

Yano, S., Kuroda, S., Shichinohe, H., Seki, T., Ohnishi, T., Tamagami, H., Hida, K., Iwasaki, Y., 2006. Bone marrow stromal cell transplantation preserves gammaaminobutyric acid receptor function in the injured spinal cord. J. Neurotrauma 23, 1682–1692.

Ying, Q.L., Nichols, J., Evans, E.P., Smith, A.G., 2002. Changing potency by spontaneous fusion. Nature 416, 545–548.

Yoshihara, H., Shumsky, J.S., Neuhuber, B., Otsuka, T., Fischer, I., Murray, M., 2006. Combining motor training with transplantation of rat bone marrow stromal cells does not improve repair or recovery in rats with thoracic contusion injuries. Brain Res. 1119, 65–75.

Zhu, H., Mitsuhashi, N., Klein, A., Barsky, L.W., Weinberg, K., Barr, M.L., Demetriou, A., Wu, G.D., 2006. The role of the hyaluronan receptor CD44 in mesenchymal stem cell migration in the extracellular matrix. Stem Cells 24, 928–935.

JOURNAL OF NEUROTRAUMA 26:1–10 (July 2009)

DOI: 10.1089/neu.2008.0776

Wnt-Ryk Signaling Mediates Axon Growth Inhibition and Limits Functional Recovery after Spinal Cord Injury

Tomohiro Miyashita,[1,2] Masao Koda,[3] Keiko Kitajo,[1] Masashi Yamazaki,[2] Kazuhisa Takahashi,[2] Akira Kikuchi,[4] and Toshihide Yamashita[1,5]

Abstract

Wnt proteins are a large family of diffusible factors that play important roles in embryonic development, including axis patterning, cell fate specification, proliferation, and axon development. It was recently demonstrated that Ryk (receptor related to tyrosine kinase) is a conserved high-affinity Wnt receptor, and that Ryk-Wnt interactions guide corticospinal axons down the spinal cord during development. Here, we report that the Ryk-Wnt signal mediates the inhibition of corticospinal axon growth in the adult spinal cord. The expression of Wnt-5a is induced in reactive astrocytes around the injury site following a spinal cord injury. *In vitro*, Wnt-5a inhibits the neurite growth of postnatal cerebellar neurons by activating RhoA/Rho-kinase. In rats with thoracic spinal cord contusion, intrathecal administration of a neutralizing antibody to Ryk resulted in significant axonal growth of the corticospinal tract and enhanced functional recovery. Thus, reexpression of the embryonic repulsive cues in adult tissues contributes to the failure of axon regeneration in the central nervous system.

Key words: axon; regeneration; Rho; spinal cord injury; Wnt

Introduction

In the adult mammalian central nervous system (CNS), it is well established that injured axons exhibit very limited regenerative ability. Due to the lack of appropriate axonal regeneration, traumatic damage to the adult brain and spinal cord frequently causes permanent neuronal deficits. After a CNS injury, various neurite outgrowth inhibitors are present around the damaged site and are considered to be, at least in part, responsible for lesion-induced poor axonal regeneration and functional deficits. Among these inhibitors, myelin-associated glycoprotein, Nogo, and oligodendrocyte-myelin glycoprotein are well characterized (Yamashita et al., 2005). Downstream of these inhibitors, the activation of RhoA and its effector Rho-associated serine/threonine kinase (Rho-kinase), after the binding of these inhibitors to the corresponding receptors, has been demonstrated to be a key element for axonal growth inhibition (Mueller et al., 2005). In addition, recent publications propose roles for other proteins, including ephrin B3, Sema4D, and repulsive guidance molecule, in inhibiting axon regeneration following spinal cord injury (SCI) (Moreau-Fauvarque et al., 2003; Benson et al., 2005; Hata et al., 2006). These proteins are well known for their ability to repel axons during the developmental stages. During the development of the nervous system, outgrowing axons are often required to travel long distances in order to reach their target neurons. In this process, outgrowing neurites tipped with motile growth cones rely on repulsive and attractive guidance cues present in their local environment. Therefore, cues that repel axons during the developmental stage may act as inhibitory molecules for injured axons in adults.

Members of the Wnt family of proteins are key regulators of pivotal developmental processes that include patterning, the specification of cell fate, and the determination of tissue polarity (Ciani et al., 2005; Zou, 2004). In recent years, evidence has accumulated to suggest that Wnt proteins also play important roles in axon development during the formation of the nervous system (Zou, 2004). Wnt proteins have been demonstrated to be bifunctional axon guidance molecules and several Wnt proteins appear to mediate guidance of corticospinal tract (CST) axons along the spinal cord via repulsion (Liu et al., 2005). Wnt-1 and Wnt-5a are expressed in the mouse spinal cord gray matter, cupping the dorsal funiculus, in an anterior-to-posterior decreasing gradient along the cervical and thoracic cord. These Wnt proteins repel CST

Departments of [1]Neurobiology and [2]Orthopaedic Surgery, Graduate School of Medicine, Chiba University, Chiba, Japan.
[3]Togane Prefectural Hospital, Chiba, Japan.
[4]Department of Biochemistry, Graduate School of Biomedical Sciences, Hiroshima University, Hiroshima, Japan.
[5]Department of Molecular Neuroscience, Graduate School of Medicine, Osaka University, Osaka, Japan.

axons *in vitro* through a conserved receptor, Ryk, which is expressed in the CST axons. The posterior growth of CST axons is blocked by a neutralizing antibody to Ryk, thereby establishing that Wnt proteins are repulsive guidance cues for developing CST axons. These findings increase the prospects of navigation for severed axons in adults, and provide evidence to suggest that some repulsive guidance cues act as inhibitors of axon growth.

In the present study, we assessed whether Wnt proteins act as inhibitors of axon growth in the adult spinal cord. The expression of Wnt-5a increased following thoracic SCI in rats. Importantly, using a function-blocking antibody, we provide evidence that Wnt-Ryk inhibition promotes axon growth and functional recovery following SCI.

Methods

All the experimental procedures were approved by the Institutional Committee of Chiba University.

Surgical procedure

Anesthetized (2% halothane) female Sprague–Dawley rats (200–250 gm) underwent a laminectomy at the T9/T10 vertebral level, thereby exposing the spinal cord. We contused the spinal cords with an Infinite Horizon Spinal Cord Impactor (Precision Systems and Instrumentation, Fairfax, VA). The impact force was set at 200 kdyn. In order to perform the neutralizing antibody treatment in the animal model, the rats were fitted with an osmotic minipump (200 μl, 0.5 μl/h, administered for 2 weeks; Alzet 2002; Durect Corp., Cupertino, CA) immediately after SCI. These pumps were filled with control rabbit immunoglobulin G (IgG; 26 animals, 13.0 μg/kg/day, over a 2-week period; Sigma, Saint Louis, MO) or an anti-Ryk antibody (21 animals, 13.0 μg/kg/day, over a 2-week period; Abgent, San Diego, CA). The anti-Ryk antibody was raised against the extracellular domain of Ryk. The minipump was placed under the skin on the animal's back, and a silastic tube connected to the outlet of the minipump was placed under the dura at the spinal cord contusion site with its tip immediately caudal to the injury site. Fibrin sealants (Beriplast; ZLB Behring, King of Prussia, PA) were allowed to drip on the dura in order to anchor the tube that was protruding from the dura. Thereafter, the muscle and skin layers were sutured. The bladder was evacuated by manual abdominal pressure at least twice a day until the bladder function was restored. Sham-operated rats ($n = 6$) underwent laminectomy at the T9/10 vertebral level, thereby exposing their spinal cords. Minipumps that were filled with 0.85% saline and connected to silastic tubes were placed in three rats. Neither a minipump nor a silastic tube was placed in the other rats. Subsequently, the muscle and skin layers were sutured.

We used a section model to examine Wnt expression. The rats received a laminectomy at vertebral level T9/10, and the spinal cord was exposed. A no. 11 blade was used for the total section of the spinal cord, and the muscle and skin layers were sutured.

Tissue preparation and immunohistochemistry

For immunohistochemistry, tissues were obtained from an uninjured spinal cord and from spinal cords at 1, 3, and 7 days after the injury. After administering deep anesthesia using sodium pentobarbital, the animals were killed by perfusion with phosphate-buffered saline (PBS) followed by 4% paraformaldehyde. The animal's spinal cords were dissected, postfixed overnight in the same fixative, and cryopreserved in 20% sucrose in PBS. The spinal cord located 5 mm rostral and 5 mm caudal to the lesion site (10 mm long) was embedded in Tissue Tek OCT and immediately frozen in liquid nitrogen at –80°C. In addition, transverse sections were also collected from the spinal cord 10 mm rostral to the injury site. Using a cryostat, a series of 50-μm parasagittal or transverse sections were cut and mounted on poly-L-lysine (PLL)-coated Superfrost-Plus slides (Matsunami, Osaka, Japan). The sections were washed three times with PBS, then blocked with PBS containing 5% bovine serum albumin (BSA) and 0.1% Triton X-100 for 1 h at room temperature. The sections were incubated overnight with primary antibody at 4°C and washed three times with PBS. This was followed by incubation with fluorescein-conjugated secondary antibody (1:1000; Molecular Probes, Eugene, OR) for 1 h at room temperature. The anti-Wnt-5a antibody was prepared in rabbits by immunizing the animals with a synthetic peptide corresponding to the mouse Wnt-5a (Kurayoshi et al., 2006). A monoclonal anti-GFAP antibody (1:200; Chemicon, Temecula, CA), the monoclonal antibody (Tuj1) that recognizes the neuron-specific β-tubulin III protein (1:500; Covance, Berkeley, CA), or the anti-Ryk antibody was used as the primary antibody.

Neurite outgrowth assay

Cerebellar granule neurons (CGNs) from postnatal rats pups (P6–P10) were dissociated by trypsinization (0.25% trypsin in PBS for 10 min at 37°C), followed by resuspension

FIG. 1. Wnt-5a is induced in astrocytes and microglia/macrophages after spinal cord injury (SCI). (**A,B**) Wnt-5a is expressed in rat spinal cord neurons. Fixed tissues were obtained for immunohistochemistry from sham-operated (control) adult rat spinal cords. Parasagittal sections were stained with the anti-Wnt-5a antibody, and double stained with the anti-Tuj1 anti-Wnt-5a antibody. Wnt-5a is expressed in the axons in the white matter and neuronal cell bodies in the gray matter. Insets of the left panel correspond to high-magnification views in the right panels (upper insets correspond to upper panels). (**C,D**) The sections were also double stained with the anti-Wnt-5a anti–glial fibrillary acidic protein (GFAP) antibody (C) or the anti-Wnt-5a anti–myelin/oligodendrocyte-specific protein (MOSP) antibody (D). Wnt-5a was not expressed in astrocytes or oligodendrocytes. (**E**) Double labeling with anti-Tuj1 and anti-Wnt-5a antibodies shows colocalization 1 day after SCI. (**F,G**) Double labeling with anti-GFAP and anti-Wnt-5a antibodies shows colocalization in the epicenter area at 1 day (F) and 7 days (G) after SCI. (**H**) Immunohistochemistry for Ryk. Axial sections of injured spinal cord 10 mm rostral to the lesion site were obtained at 7 days after SCI, and were immunostained with the anti-Ryk antibody. The immunoreactivity for Ryk was found in the ventral part of the dorsal column. An inset of the left panel corresponds to a high-magnification view of the dorsal corticospinal tract (CST) in the right panel. Scale bar = 500 μm (left-side panels); 100 μm (right panel of H); 50 μm (others).

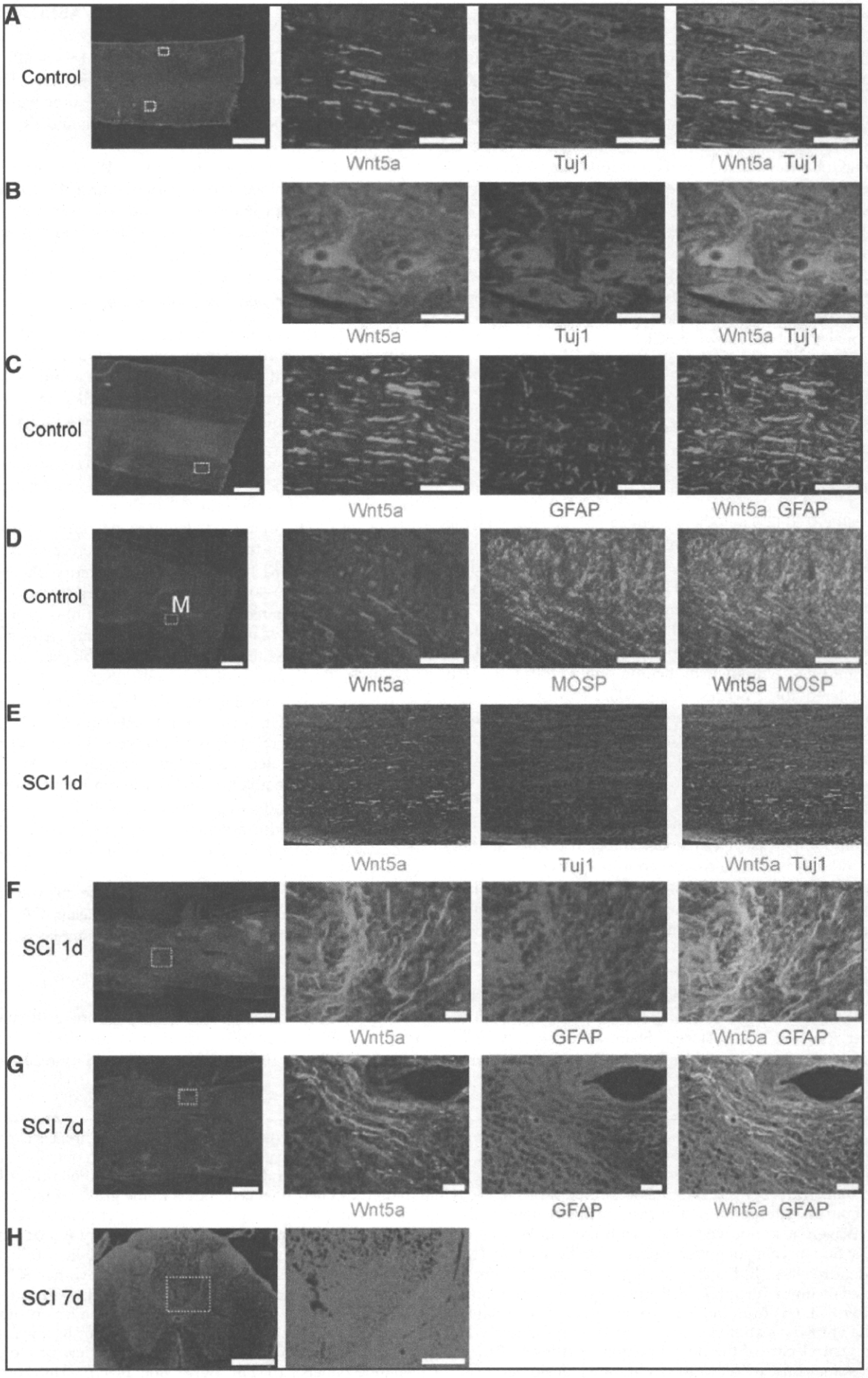
A
Control
Wnt5a
Tuj1
Wnt5a Tuj1
B
Wnt5a
Tuj1
Wnt5a Tuj1
C
Control
Wnt5a
GFAP
Wnt5a GFAP
D
Control
M
Wnt5a
MOSP
Wnt5a MOSP
E
SCI 1d
Wnt5a
Tuj1
Wnt5a Tuj1
F
SCI 1d
Wnt5a
GFAP
Wnt5a GFAP
G
SCI 7d
Wnt5a
GFAP
Wnt5a GFAP
H
SCI 7d

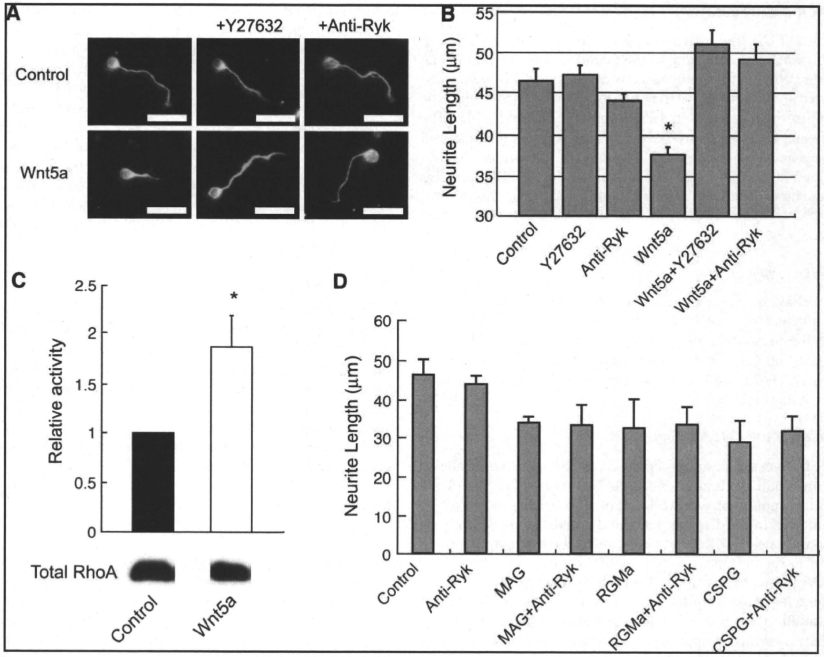

FIG. 2. Wnt proteins inhibit cerebellar granule neuron (CGN) neurite outgrowth. (**A**) CGNs were cultured on poly-L-lysine (PLL)–coated chamber slides for 24 h in a conditioned media with or without soluble Wnt-5a (90 ng/ml). Where indicated, Y27632 (10 μM) or the anti-Ryk antibody (0.5 μg/ml) was added. Scale bar = 25 μm. (**B**) The mean length of the longest neurite per neuron. The soluble form of Wnt-5a inhibits neurite outgrowth by a Rho-kinase-dependent mechanism and the anti-Ryk antibody reverses the effect of Wnt-5a. $^*P < 0.01$ (one-way analysis of variance [ANOVA] followed by Scheffe's multiple comparison test). Data are represented as the mean ± standard error of the mean (SEM) of three independent experiments. (**C**) Wnt-5a activates RhoA in the CGNs. CGNs were treated for 10 min with soluble Wnt-5a (90 ng/ml). The active fraction of RhoA was detected by a G-LISA Rho activation assay and the relative activity is shown. The bottom panel shows a western blot for total RhoA in the lysates. $^*P < 0.05$ (Student's *t*-test). Data are represented as the mean ± SEM of four independent experiments. (**D**) The anti-Ryk antibody does not abolish the effect of MAG, RGMa, or chondroitin sulfate proteoglycans (CSPG). The mean length of the longest neurite per neuron. CGNs were cultured on PLL-coated chamber slides for 24 h in a conditioned media with or without soluble MAG-Fc (20 μg/ml), RGMa (2 μg/ml), or CSPG (1 μg/ml).

in a serum-containing medium, trituration, and three washes with PBS. The cultures were grown in serum-free Dulbecco's modified Eagle's medium (DMEM). For the soluble Wnt-5a assays, neurons were plated on a conditioned media on PLL-coated chamber slides (Lab-Tek; Nalge Nunc International, Rochester, NY) and incubated for 24 h. Wnt-5a proteins were purified to near homogeneity by three successive column chromatographies (Kishida et al., 2004; Kurayoshi et al., 2006). The concentration of Wnt-5a were 90 ng/ml. Where indicated, 10 μM Y27632 (Mitsubishi Pharmaceuticals, Tokyo, Japan) was added to the cultures. For the neutralizing antibody assay, the anti-Ryk antibody (Abgent) was added to the culture at a concentration of 0.5 μg/ml. Where indicated, rat MAG-Fc chimera (25 μg/ml; R&D Systems), chicken extracellular chondroitin sulfate proteoglycans (CSPGs; the major components of this mixture are neurocans, phosphacan, versican, and aggrecan; Chemicon), or recombinant mouse RGMa (1 μg/ml; R&D Systems) were added. The cells were fixed in 4% (wt/vol) paraformaldehyde and immunostained with a monoclonal antibody (Tuj1) that recognized the neuron-specific β-tubulin III protein (1:1000; Covance). Subsequently, the length of the longest neurite for each β-tubulin III-positive neuron was determined. The neurite length of 100 neurons was measured for each experiment ($n = 3$).

RhoA activity assay

A G-LISA Rho activation assay kit (Cytoskeleton, Denver, CO) was used according to the manufacturer's recommendations. Where indicated, the cultures of the CGNs were incubated with Wnt-5a (90 ng/ml) for 10 min after which the cultures were grown in serum-free DMEM for 12–24 h. The protein concentrations of the cell lysates were equalized between 1.0 and 2.0 mg/ml. The surplus cell lysates were retained for further assay. The amount of the total Rho proteins was determined by western blotting using a monoclonal antibody against RhoA (Santa Cruz Biotechnology, Santa Cruz, CA).

Behavioral testing

Behavioral recovery was assessed in an open-field environment for 8 weeks after the injury by using the Basso-Beattie-Bresnahan (BBB) locomotor rating scale (Basso et al., 1995). Uninjured and sham-operated rats ($n = 6$) achieved full scores. The quantification was performed in a blinded manner by two observers.

Anterograde CST labeling

Six weeks after injury, descending CST fibers were labeled with biotin dextran amine (BDA), 10% in saline, 2.0 μl per cortex (molecular weight [MW] of 10,000; Molecular Probes) that was injected in the left motor cortex under anesthesia (coordinates: 0.5–2.5 mm posterior to the bregma, 2 mm lateral to the bregma, 1.5-mm depth). For each injection, 0.5 μl BDA was delivered for a 30-s period via a 15–20-μm internal diameter glass capillary attached to a microliter syringe (Hamilton, Reno, NV). In total, we examined and compared the regenerative responses of four control and seven anti-Ryk antibody-treated rats after SCI. The animals were killed by perfusion with PBS followed by 4% paraformaldehyde 14 d after the BDA injection. The animal's spinal cords were dissected, postfixed overnight in the same fixative, and cryopreserved in 20% sucrose in PBS. The spinal cord located between 5 mm rostral and 5 mm caudal to the lesion site (10-mm long) was embedded in Tissue Tek OCT. These blocks were sectioned (50 μm) in the sagittal or transverse plane, retaining each section. In both cases, the transverse sections were also collected from the spinal cord located more than 5 mm rostral and caudal to the injury site (15 control and 13 anti-Ryk antibody-treated rats). We used the transverse sections for quantification, and the sagittal sections for the presentation of the images. These sections were incubated for 1 h with Alexa Fluor 488-conjugated streptavidin (1:400; Molecular Probes) in PBS containing 0.05% Tween-20.

Data analysis

Fifty-micrometer-thick transverse sections (four control and seven anti-Ryk antibody-treated rats) were evaluated. For each section, the number of intersections of BDA-labeled fibers was counted from 4 mm above to 4 mm below the lesion site. The axon number was calculated as the percentage of the fibers observed 4 mm above the lesion, where the CST was intact. The distance beyond the epicenter of the lesion was scored as a positive distance, whereas the other regions were scored as negative distances.

Results

Expression of Wnt-5a in the adult rat spinal cord

We first investigated the distribution pattern of Wnt proteins in the adult rat spinal cord. We performed immunohistochemistry on fixed sections of uninjured spinal cords. In the uninjured spinal cord of adult rats, immunoreactivity to Wnt-5a was observed in the white matter and the signal was colocalized with the immunoreactivity to neuron-specific ß-tubulin III protein (Tuj1) (Fig. 1A), demonstrating that Wnt-5a was expressed in the spinal cord axons. The Wnt-5a

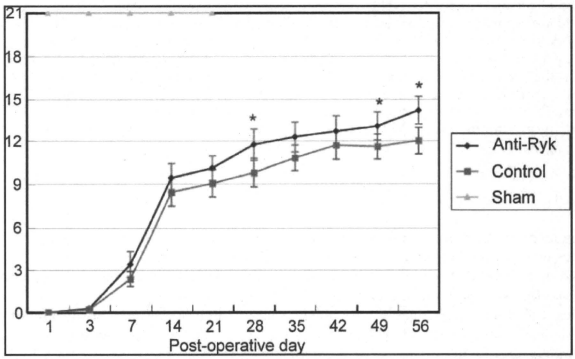

FIG. 3. The anti-Ryk antibody promotes locomotor recovery after spinal cord injury (SCI). The Basso-Beattie-Bresnahan (BBB) score was determined at the indicated times after thoracic contusion in the anti-Ryk antibody-treated (Anti-Ryk), control immunoglobulin G (IgG)–treated (Control), and sham-operated (Sham) rats. The mean ± standard error of the mean (SEM) of 21, 26, and six rats for each group, respectively. As indicated, the anti-Ryk antibody-treated group is statistically different from the control group. *$P < 0.05$ (Student's t-test) compared with the control.

immunoreactivity was also observed in the somata of Tuj1-positive neurons in the gray matter (Fig. 1B). Double immunostaining with the anti-Wnt-5a antibody and an antibody against the glial fibrillary acidic protein (GFAP) revealed no colocalization, demonstrating that Wnt-5a was not present in astrocytes (Fig. 1C). Double staining using anti-Wnt-5a anti–myelin/oligodendrocyte-specific protein (MOSP) antibodies demonstrated that Wnt-5a was not expressedin oligodendrocytes (Fig. 1D). Thus, Wnt-5a was expressed in neurons in the adult rat spinal cord.

Expression of Wnt-5a is up-regulated following SCI

In order to address whether Wnt proteins play a role in pathogenesis after CNS injury, we examined Wnt-5a expression following SCI in rats. We performed immunohistochemistry on fixed sections obtained at 1, 3, and 7 days after injury at the T9/10 vertebral level. Immunoreactivity to Wnt-5a was induced around the injury site during the observation period following surgery. We performed a double-label experiment after the injury to characterize the Wnt-5a-expressing cells. GFAP-positive and Wnt-5a-positive cells were detected in the epicenter area 1 day (Fig. 1F) and 7 days (Fig. 1G) after SCI, suggesting that Wnt-5a is expressed in the reactive astrocytes at the lesion epicenter. Immunoreactivity to Wnt-5a was observed in the white matter and the signal was colocalized with the immunoreactivity to Tuj1 (Fig. 1E). We did not observe MOSP-positive/Wnt-5a-positive cells in the lesion epicenter or in the adjacent white matter (data not shown), suggesting that oligodendrocytes do not express Wnt-5a.

We then obtained axial sections from injured spinal cord 10 mm rostral to the lesion site and assessed whether one of the receptors for Wnts (Ryk) was expressed in the spinal cord. The immunoreactivity for Ryk was found in the ventral part of the dorsal column—where the dorsal CST runs—at 7 days after SCI (Fig. 1H), although we found no significant immunoreactivity for Ryk in the dorsal column in the sham-operated rats (data not shown). These findings suggest that Ryk was expressed in the proximal axons of the CST after injury, which is consistent with the previous report (Liu et al., 2008).

Wnt-5a inhibits neurite outgrowth by a mechanism dependent on Ryk in vitro

A possible role of Wnt proteins in the pathogenesis of SCI is that they contribute to axonal inhibition. In order to address this hypothesis *in vitro*, we employed CGNs obtained from postnatal rats (P6–P10). These cells are frequently used for studying the function of the molecules that inhibit neurite growth (Yamashita et al., 2005). Although neurons from the adult cerebral cortex may be the optimal system for this type of study, to date we have been unsuccessful in culturing these neurons *in vitro*. For use in this assay, the Wnt-5a protein was purified to near homogeneity by three successive column chromatographies (Kishida et al., 2004; Kurayoshi et al., 2006). The CGNs from postnatal rats were cultured on PLL-coated slides in the presence or absence of Wnt-5a. At a concentration of 90 ng/ml, Wnt-5a significantly inhibited the neurite outgrowth of the CGNs (Fig. 2A,B). This inhibitory effect depended on Rho-kinase since the treatment of the CGNs with 10 μM Y27632—a specific inhibitor of Rho-associated protein kinase p160 ROCK (Uehata et al., 1997)—attenuated the effect of Wnt-5a, whereas Y27632 alone had no effect on neurite growth (Fig. 2A,B). To our knowledge, this is the first report to suggest that Wnt-5a inhibits neurite outgrowth, presumably by activating RhoA/Rho-kinase. Therefore, to directly assess whether RhoA is involved in the effect of Wnt-5a, the activity of RhoA was determined using the RhoA-binding domain of the effector protein, Rhotekin (Ren et al., 1999) and the G-LISA assay system (Fig. 2C). The assay revealed that, within 10 min of the addition of soluble Wnt-5a, extracts of the cells contained increased amounts of GTP-RhoA compared to those of the control cells. These results strongly suggest that Wnt-5a inhibits neurite outgrowth by a mechanism dependent on the activation of the RhoA/Rho-kinase pathway.

Ryk is a high-affinity receptor for Wnt-1, Wnt-3a, and Drosophila Wnt-5 (Yoshikawa et al., 2003; Lu et al., 2004). Ryk has been demonstrated to transmit repulsive signals in neurons (Liu et al., 2005; Schmitt et al., 2006; Keeble et al., 2006). This receptor is expressed in CGNs at a corresponding age (P6–P10) (Kamitori et al., 1999). These findings prompted us to examine whether Ryk is involved in the Wnt-mediated inhibition of CGN neurite growth. We used a polyclonal antibody for the ectodomain of Ryk (anti-Ryk) and tested whether the anti-Ryk antibody could block Wnt-5a-mediated inhibition. We observed that the addition of the anti-Ryk antibody (0.5 μg/ml) efficiently blocked the inhibitory effects of Wnt-5a at a concentration of 90 ng/ml (Fig. 2A,B), whereas the anti-Ryk antibody alone had no effect on neurite growth. However, the anti-Ryk antibody (0.5 μg/ml) did not influence the inhibitory effect of other neurite growth inhibitors, including MAG, RGMa, or CSPG (Fig. 2D), demonstrating the specificity of this neutralizing antibody. Therefore, Ryk is

FIG. 4. The anti-Ryk antibody promotes the regeneration/sprouting of corticospinal tract (CST) axons after spinal cord injury (SCI). (**A,C,E,G**) Representative transverse sections of the spinal cord located 10 mm rostral to the lesion site in the anti-Ryk antibody-treated (A,C) and control immunoglobulin G (IgG)–treated (E,G) rats. (C,G) Insets of (A) and (E), respectively, show high-magnification views of the dorsal CST. (**B,F**) Representative pictures of the spinal cord at 8 weeks after injury; the rostral site is indicated to the left. The anti-Ryk antibody-treated (B) or control IgG-treated (F) spinal cord at 8 weeks after the injury. (**D,H**) Higher magnifications of the boxed regions in (B) and (F), respectively. Anterograde-labeled CST fibers were observed caudally in rats treated with the anti-Ryk antibody (D), but not in the corresponding regions of the control IgG-treated rats (H). Scale bar = 500 μm (A,B,E,F); 200 μm (C,D,G,H). (**I**) The number of labeled corticospinal axons located 10 mm rostral to the lesion site in rats treated with the control IgG or the anti-Ryk antibody was measured by using the transverse sections. No significant difference was observed. (**J**) Quantification of the labeled CST fibers in seven anti-Ryk-treated and four control IgG-treated animals. Fifty-micrometer-thick transverse sections were evaluated. The *x*-axis indicates specific locations along the rostrocaudal axis of the spinal cord. The *y*-axis indicates the ratio of the number of biotin dextran amine (BDA)–labeled fibers at the indicated site to those at 4 mm rostral to the lesion site. $^*P < 0.01$ compared with the control (Student's *t*-test).

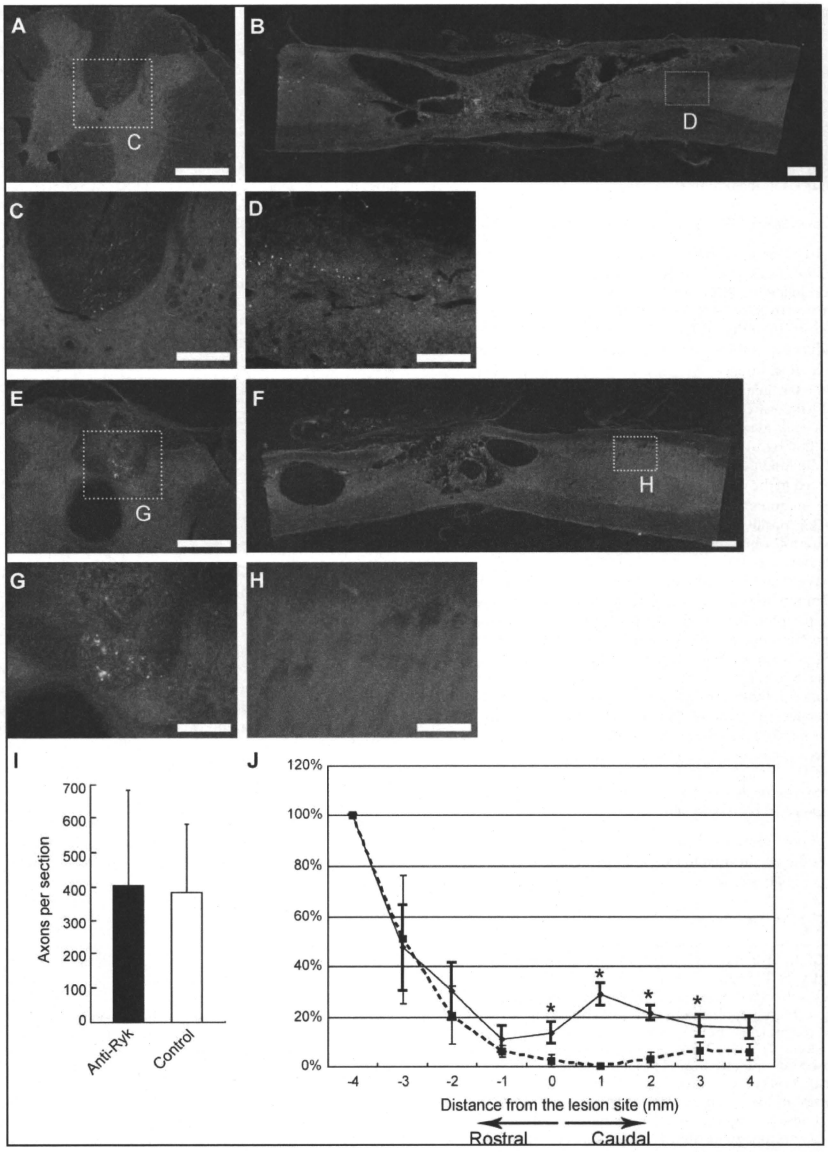
A
B
C
D
C
D
E
F
G
H
G
H
I
Axons per section
700
600
500
400
300
200
100
0
Anti-Ryk
Control
J
120%
100%
80%
60%
40%
20%
0%
-4
-3
-2
-1
0
1
2
3
4
Distance from the lesion site (mm)
Rostral
Caudal

required for the inhibitory effect of Wnt-5a on CGN neurite growth.

Ryk neutralization leads to functional improvement

The binding of Wnts to Ryk repels CST axons during the developmental stages both *in vitro* and *in vivo* (Liu et al., 2005), and Ryk is expressed in the CST of adult rats after SCI (Fig. 1X,Y). The above-mentioned results suggest the possibility that Wnt proteins, by virtue of their ability to inhibit neurite outgrowth, act as a barrier to the regrowth of injured axons after SCI, and that the blockage of these proteins may enhance recovery after SCI. We employed a rat spinal contusion model since this is relevant to clinical conditions. The spinal cords at the thoracic level (Th9/10) were contused by an impactor. The anti-Ryk antibody or a rabbit IgG control was administered for 2 weeks via osmotic minipumps connected to intrathecal catheters placed near the thoracic injury site. The locomotor performance of the animals was monitored over an 8-week period after the injury. The sham-operated rats (Fig. 3) achieved full scores according to the BBB locomotor rating scale (Basso et al., 1995). All rats with a SCI became almost completely paraplegic from days 1–3 after the injury. As indicated by their BBB scores, these animals gradually exhibited partial recovery of locomotor behavior (Fig. 3). At 2–8 weeks after the injury, the locomotor performance of rats treated with the anti-Ryk antibody tended to exhibits a better recovery than in those treated with the control IgG. On average, the control IgG-treated rats attained a BBB score of 12.0, whereas those treated with the anti-Ryk antibody achieved a significantly higher BBB score of 14.2 at 8 weeks after the surgery (Fig. 3). Thus, the anti-Ryk antibody treatment significantly improved locomotor recovery following the spinal cord contusion in rats.

Ryk inhibition induces growth of injured corticospinal fiber tracts

Finally, we examined whether Wnt-Ryk signaling contributes to the inhibition of axon regeneration/sprouting after the SCI. The integrity of the dorsal CST in previously tested rats was assessed by injecting BDA into the unilateral sensorymotor cortex. The total number of labeled fibers located 10 mm above the lesion was not different between the anti-Ryk antibody-treated and the control IgG-treated rats (Fig. 4A,C,E,G,I), thus indicating that the extent of BDA uptake was identical between the groups. For a group of animals (four control and seven anti-Ryk antibody-treated rats), blocks that extended 5 mm rostral and 5 mm caudal to the center of the injury were sectioned in the sagittal plane (Fig. 4B,F). It is notable that labeled fibers with typical irregular meandering growth patterns were frequently observed in the tissue caudal to the lesion in the anti-Ryk antibody-treated rats (Fig. 4B,D), whereas no BDA-labeled CST fibers were detected in the control IgG-treated rats (Fig. 4F,H). We then reconstructed the transverse sections of the injured spinal cord and estimated the number of labeled fibers. Compared to the number of labeled fibers that were observed 4 mm rostral to the lesion site, more than 20% of the labeled fibers were observed 1–2 mm caudal to the lesion epicenter in the anti-Ryk antibody-treated rats. However, only a small percentage of the labeled fibers (0% at 1 mm and 3% at 2 mm caudal to the injury site) were observed in the control IgG-treated rats (Fig. 4J). Labeled fibers were detected in the gray matter of injured animals treated with the anti-Ryk antibody (Fig. 4D). Since we observed no labeled fibers in the normal locations of the dorsal CST caudal to the lesion site in any of the injured rats (data not shown), the increase in the labeled fibers after the anti-Ryk antibody treatment was not due to an increased survival of the dorsal CST. Thus, these results demonstrate that treatment with the anti-Ryk antibody promoted significant fiber growth from the intact ventral CST or the injured dorsal CST after SCI. Ryk appears to mediate the inhibition of CST axon growth following SCI.

Discussion

Our study demonstrates that Wnt-5a was induced in the reactive astrocytes surrounding the site of injury after SCI in rats. Importantly, continuous infusion of the anti-Ryk antibody by osmotic minipumps resulted in the enhancement of the locomotor activity as well as the sprouting of the labeled CST. As our *in vitro* data demonstrate that neurite growth inhibition mediated by Wnt-5a is dependent on Rho-kinase, and that Wnt-5a activated RhoA in the CGNs, it is suggested that RhoA/Rho-kinase plays a role in the Wnt-mediated inhibition of axon growth *in vivo*.

Intracellular signals of axon growth inhibitors converge at RhoA and Rho-kinase

Several proteins in the CNS have been identified as inhibitors of axonal regeneration following the injury to the CNS in adult vertebrates. Three major inhibitors, Nogo, myelin-associated glycoprotein, and oligodendrocyte-myelin glycoprotein—expressed by oligodendrocytes and myelinated fiber tracts—have been identified (Yamashita et al., 2005). All these inhibitors were observed to bind to the Nogo receptor in complex with p75 or TROY, members of the TNF receptor family, and LINGO-1. The ligands binding to this receptor complex induce activation of RhoA and Rho-kinase and this signal transduction is necessary for axonal growth inhibition, at least *in vitro* (Mueller et al., 2005). Other studies have demonstrated that neurite outgrowth inhibitors, such as CSPG, and members of the semaphorin, ephrin, and repulsive guidance molecule families, also utilize the RhoA/Rho-kinase pathway for their inhibitory functions (Mueller et al., 2005). Our study demonstrates that the inhibitory effects of Wnt-5a depended on Rho-kinase *in vitro*, and that RhoA was activated in the CGNs when treated with Wnt-5a. Previous observations have demonstrated that these Wnts signal through RhoA and Rho-kinase. Activation of Rho-kinase by Wnt-3a induces neurite retraction from N1E-115 neuroblastoma cells (Kishida et al., 2004). Furthermore, a genetic study using zebrafish embryos demonstrated that the disruption of convergence and extension movement in *Wnt-5* or *Wnt-1* mutants was rescued by ectopic expression of RhoA or Rho-kinase, suggesting that RhoA/Rho-kinase act downstream of these Wnts (Zhu et al., 2005). Therefore, Wnt proteins expressed in cells surrounding the injured site may limit axon growth by activating RhoA/Rho-kinase in the neurons after SCI. Our findings suggest new candidates for the role of inhibitors of axon regeneration, which presumably employ common signaling.

Glial cells express axon growth inhibitors

In this study, we observed the induced expression of Wnt-5a in the reactive astrocytes surrounding the injury site

after SCI. CNS myelin derived from oligodendrocytes was first postulated as a major source of inhibition and several myelin-associated components that can inhibit axon outgrowth *in vitro* have been identified. In addition to the three above-mentioned myelin-derived inhibitors, the transmembrane semaphorin 4D (Moreau-Fauvarque et al., 2003), ephrin B3 (Benson et al., 2005), and repulsive guidance molecule (Hata et al., 2006) were proposed as members of the myelin-derived inhibitors. It is clear that CNS myelin exerts multiple layers of inhibitory influences *in vivo* as well as *in vitro* (Yamashita et al., 2005), although the extent of the relative contribution of each molecule remains to be determined. In addition to myelin, another important source of inhibition is the glial scar that forms after CNS injury. Many astrocytes in the injured area often become hypertrophic and adopt a reactive phenotype, releasing CSPG (McKeon et al., 1991). After injury, CSPG expression is rapidly up-regulated by reactive astrocytes, forming an inhibitory gradient that is highest at the center of the lesion. The intrathecal administration of chondroitinase ABC—an enzyme that removes GAG chains from the protein core—following SCI promoted the regeneration of various axon tracts as well as functional recovery (Bradbury et al., 2002; Moon et al., 2001). In addition, mutant mice that are deficient in both GFAP and vimentin exhibit reduced astroglial reactivity and this results in supraspinal sprouting and functional recovery after SCI (Menet et al., 2003), supporting the supposition that astrocytes may contribute to the inability of the injured spinal cord to regenerate. Therefore, our data, in combination with these findings, suggest that multiple inhibitors expressed in the reactive astrocytes, as well as myelin from the oligodendrocytes, may constitute a barrier that inhibits axon sprouting and functional recovery.

Multiple molecular targets for the treatment of SCI

Liu et al. (2008) reported that Wnt1 and Wnt5a were induced in the gray matter after unilateral hemisection of the spinal cord. Ryk was also induced in the CST axons. Injection of function blocking antibody to Ryk into the dorsal bilateral hemisectioned spinal cord prevented the retraction of CST axons or promoted growth of CST. Our results are consistent with these observations, although we have novel data, including *in vitro* experiments. Importantly, we observed improvement of the locomotor function after spinal contusion, which is more relevant to clinical conditiones, by the anti-Ryk antibody treatment. Although a growing number of candidate molecules are suggested to be implicated in the inhibition of the regeneration of injured CNS axons, the extent of the relative contribution of each molecule remains to be determined. Combination therapies designed to target multiple inhibitors may be more effective than those that target an individual component. As many of these inhibitors utilize common signals, such as RhoA/Rho-kinase, for axon growth inhibition, it may be postulated that the inhibition of RhoA or Rho-kinase would be one of the most effective approaches for the treatment of SCI patients. Indeed, the pharmacological inhibition of RhoA or Rho-kinase has been demonstrated to promote axon growth and locomotor activity (Dergham et al., 2002; Fournier et al., 2003; Hara et al., 2000; Sung et al., 2003; Tanaka et al., 2004). However, it should be noted that pharmacological inhibitors are not cell type specific and, therefore, act not only on neurons but also on other cell types, including astrocytes and oligodendrocytes. Anti-Ryk antibody treatment for the first 2 weeks was sufficient in our study, and this is the case for the Rho-kinase inhibitor treatment (Tanaka et al., 2004). Therefore, there seems to be some critical therapeutic period for the treatment of SCI. It is important to elucidate the whole network of the signal transduction mechanism of axon growth inhibition; therefore, our study provides evidence for a promising molecular target for the treatment of SCI.

Our observations strongly suggest that Wnt-Ryk signalling contributes significantly to the inability of the adult CNS to regenerate after injury. Although the CST axons are propelled down the spinal cord by a gradient of Wnt-1 and Wnt-5a acting through Ryk during the developmental stage, the severed CST axons in adults are stunted by the Wnt-Ryk signalling. The anti-Ryk antibody provides an effective therapeutic strategy for the treatment of CNS injury.

Acknowledgments

This work was supported by a Research Grant from National Institute of Biomedical Innovation (05–12) and Grant-in-Aid for Young Scientists (from JSPS to T.Y.).

Author Disclosure Statement

No competing financial interests exist.

References

Basso, D.M., Beattie, M.S., and Bresnahan, J.C. (1995). A sensitive and reliable locomotor rating scale for open field testing in rats. J. Neurotrauma 12, 1–21.

Benson, M.D., Romero, M.I., Lush, M.E., Lu, Q.R., Henkemeyer, M., and Parada, L.F. (2005). Ephrin-B3 is a myelin-based inhibitor of neurite outgrowth. Proc. Natl. Acad. Sci. USA 102, 10694–10699.

Bradbury, E.J., Moon, L.D., Popat, R.J., King, V.R., Bennett, G.S., Patel, P.N., Fawcett, J.W., and McMahon, S.B. (2002). Chondroitinase ABC promotes functional recovery after spinal cord injury. Nature 416, 636–640.

Ciani, L., and Salinas, P.C. (2005). WNTs in the vertebrate nervous system: from patterning to neuronal connectivity. Nat. Rev. Neurosci. 6, 351–362.

Dergham, P., Ellezam, B., Essagian, C., Avedissian, H., Lubell, W.D., and McKerracher, L. (2002). Rho signaling pathway targeted to promote spinal cord repair. J. Neurosci. 22, 6570–6577.

Fournier, A.E., Takizawa, B.T., and Strittmatter, S.M. (2003). Rho kinase inhibition enhances axonal regeneration in the injured CNS. J. Neurosci. 23, 1416–1423.

Hara, M., Takayasu, M., Watanabe, K., Noda, A., Takagi, T., Suzuki, Y., and Yoshida, J. (2000). Protein kinase inhibition by fasudil hydrochloride promotes neurological recovery after spinal cord injury in rats. J. Neurosurg. 93, 94–101.

Hata, K., Fujitani, M., Yasuda, Y., Doya, H., Saito, T., Yamagishi, S., Mueller, B.K., and Yamashita, T. (2006). RGMa inhibition promotes axonal growth and recovery after spinal cord injury. J. Cell Biol. 173, 47–58.

Kamitori, K., Machide, M., Osumi, N., and Kohsaka, S. (1999). Expression of receptor tyrosine kinase RYK in developing rat central nervous system. Brain Res. Dev. Brain Res. 114, 149–160.

Keeble, T.R., Halford, M.M., Seaman, C., Kee, N., Macheda, M., Anderson, R.B., Stacker, S.A., and Cooper, H.M. (2006). The Wnt receptor Ryk is required for Wnt-5a-mediated axon

guidance on the contralateral side of the corpus callosum. J. Neurosci. 26, 5840–5848.

Kishida, S., Yamamoto, H., and Kikuchi, A. (2004). Wnt-3a and Dvl induce neurite retraction by activating Rho-associated kinase. Mol. Cell Biol. 24, 4487–4501.

Kurayoshi, M., Oue, N., Yamamoto, H., Kishida, M., Inoue, A., Asahara, T., Yasui, W., and Kikuchi, A. (2006). Expression of Wnt-5a is correlated with aggressiveness of gastric cancer by stimulating cell migration and invasion. Cancer Res. 66, 10439–10448.

Liu, Y., Shi, J., Lu, C.C., Wang, Z.B., Lyuksyutova, A.I., Song, X.J., and Zou, Y. (2005). Ryk-mediated Wnt repulsion regulates posterior-directed growth of corticospinal tract. Nat. Neurosci. 8, 1151–1159.

Liu, Y., Wang, X., Lu, C.C., Kerman, R., Steward, O., Xu, X.M., and Zou, Y. (2008). Repulsive Wnt signaling inhibits axon regeneration after CNS injury. J. Neurosci. 28, 8376–8382.

Lu, W., Yamamoto, V., Ortega, B., and Baltimore, D. (2004). Mammalian Ryk is a Wnt coreceptor required for stimulation of neurite outgrowth. Cell 119, 97–108.

McKeon, R.J., Schreiber, R.C., Rudge, J.S., and Silver, J. (1991). Reduction of neurite outgrowth in a model of glial scarring following CNS injury is correlated with the expression of inhibitory molecules on reactive astrocytes. J. Neurosci. 11, 3398–3411.

Menet, V., Prieto, M., Privat, A., and Gimenez y Ribotta, M. (2003). Axonal plasticity and functional recovery after spinal cord injury in mice deficient in both glial fibrillary acidic protein and vimentin genes. Proc. Natl. Acad. Sci. USA 100, 8999–9004.

Moon, L.D., Asher, R.A., Rhodes, K.E., and Fawcett, J.W. (2001). Regeneration of CNS axons back to their target following treatment of adult rat brain with chondroitinase ABC. Nat. Neurosci. 4, 465–466.

Moreau-Fauvarque, C., Kumanogoh, A., Camand, E., Jaillard, C., Barbin, G., Boquet, I., Love, C., Jones, E.Y., Kikutani, H., Lubetzki, C., Dusart, I., and Chedotal, A. (2003). The transmembrane semaphorin Sema4D/CD100, an inhibitor of axonal growth, is expressed on oligodendrocytes and upregulated after CNS lesion. J. Neurosci. 23, 9229–9239.

Mueller, B.K., Mack, H., and Teusch, N. (2005). Rho kinase, a promising drug target for neurological disorders. Nat. Rev. Drug Discov. 4, 387–398.

Ren, X.D., Kiosses, W.B., and Schwartz, M.A. (1999). Regulation of the small GTP-binding protein Rho by cell adhesion and the cytoskeleton. Embo. J. 18, 578–585.

Schmitt, A.M., Shi, J., Wolf, A.M., Lu, C.C., King, L.A., and Zou, Y. (2006). Wnt-Ryk signalling mediates medial-lateral retinotectal topographic mapping. Nature 439,31–37.

Sung, J.K., Miao, L., Calvert, J.W., Huang, L., Louis Harkey, H., and Zhang, J.H. (2003). A possible role of RhoA/Rho-kinase in experimental spinal cord injury in rat. Brain Res. 959, 29–38.

Tanaka, H., Yamashita, T., Yachi, K., Fujiwara, T., Yoshikawa, H., and Tohyama, M. (2004). Cytoplasmic p21(Cip1/WAF1) enhances axonal regeneration and functional recovery after spinal cord injury in rats. Neuroscience 127, 155–164.

Uehata, M., Ishizaki, T., Satoh, H., Ono, T., Kawahara, T., Morishita, T., Tamakawa, H., Yamagami, K., Inui, J., Maekawa, M., and Narumiya, S. (1997). Calcium sensitization of smooth muscle mediated by a Rho-associated protein kinase in hypertension. Nature 389, 990–994.

Yamashita, T., Fujitani, M., Yamagishi, S., Hata, K., and Mimura, F. (2005). Multiple signals regulate axon regeneration through the Nogo receptor complex. Mol. Neurobiol. 32, 105–112.

Yoshikawa, S., McKinnon, R.D., Kokel, M., and Thomas, J.B. (2003). Wnt-mediated axon guidance via the Drosophila Derailed receptor. Nature 422, 583–588.

Zhu, S., Liu, L., Korzh, V., Gong, Z., and Low, B.C. (2005). RhoA acts downstream of Wnt5 and Wnt11 to regulate convergence and extension movements by involving effectors Rho kinase and Diaphanous: use of zebrafish as an in vivo model for GTPase signaling. Cell Signal. 18, 359–372.

Zou, Y. (2004). Wnt signaling in axon guidance. Trends. Neurosci. 27, 528–532.

Address reprint requests to:
Toshihide Yamashita, M.D., Ph.D.
Department of Molecular Neuroscience
Graduate School of Medicine
Osaka University
2-2 Yamadaoka, Suita
Osaka 565-0871, Japan

E-mail: yamashita@molneu.med.osaka-u.ac.jp

Acta Neuropathol
DOI 10.1007/s00401-008-0476-x

ORIGINAL PAPER

Deletion of macrophage migration inhibitory factor attenuates neuronal death and promotes functional recovery after compression-induced spinal cord injury in mice

Yutaka Nishio · Masao Koda · Masayuki Hashimoto · Takahito Kamada · Shuhei Koshizuka · Katsunori Yoshinaga · Shin Onodera · Jun Nishihira · Akihiko Okawa · Masashi Yamazaki

Received: 13 August 2008 / Revised: 16 December 2008 / Accepted: 20 December 2008

Abstract Macrophage migration inhibitory factor (MIF) is a multipotential protein that acts as a proinflammatory cytokine, a pituitary hormone, and a cell proliferation and migration factor. The objective of this study was to elucidate the role of MIF in spinal cord injury (SCI) using female MIF knockout (KO) mice. Mouse spinal cord compression injury was produced by application of a static load (T8 level, 20 g, 5 min). We analyzed the motor function of the hind limbs and performed histological examinations. Hind-limb function recovered significantly in the KO mice starting from three weeks after injury. Cresyl-violet staining revealed that the number of surviving neurons in the KO mice was significantly larger than that of WT mice six weeks after injury. Immunohistochemical analysis revealed that the number of NeuN/caspase-3-active, double-positive, apoptotic neurons in the KO mice was significantly smaller than that of the WT mice 24 and 72 h after SCI. These results were related to in-vitro studies showing increased resistance of cerebellar granular neurons from MIF-KO animals to glutamate neurotoxicity. These results suggest that MIF existence hinders neuronal survival after SCI. Suppression of MIF may attenuate detrimental secondary molecular responses of the injured spinal cord.

Keywords Macrophage migration inhibitory factor · Spinal cord injury · Glutamate · Apoptosis · Knockout mouse

Y. Nishio · M. Koda · M. Hashimoto (✉) · T. Kamada · S. Koshizuka · K. Yoshinaga · A. Okawa · M. Yamazaki
Department of Orthopaedic Surgery,
Graduate School of Medicine, Chiba University,
1-8-1 Inohana, Chuo-ku, Chiba 260-8670, Japan
e-mail: futre@tg7.so-net.ne.jp

S. Onodera
Department of Sports Medicine and Joint Reconstruction Surgery,
Graduate School of Medicine, Hokkaido University,
North 15 West 7, Kita-ku, Sapporo 060-8638, Japan

J. Nishihira
Department of Medical Bioinformatics,
Hokkaido Information University, 59-2 Nishinopporo,
Ebetsu, Hokkaido 069-8585, Japan

Published online: 06 January 2009

Introduction

Macrophage migration inhibitory factor (MIF) is a T-cell-derived, soluble lymphokine [4]. MIF was originally found to inhibit the migration of macrophages and activate them at inflammatory loci. Furthermore, MIF functions as a hormone and immunomodulator, and as a proinflammatory cytokine, and has been identified in many organs (e.g., brain, kidney, and liver [11]).

In the normal central nervous system (CNS), MIF is found in astrocytes, ependymal cells, and epithelial cells of the choroid plexus [12]. It increases in cerebrospinal fluid soon after SCI in rats [7] and increases significantly in the cerebrospinal fluid of patients with multiple sclerosis and neuro-Behçet's disease [10]. Previously we reported in detail on the upregulation of MIF after SCI [9]. MIF mRNA is upregulated in microglia accumulating in the lesion epicenter three days after SCI and in astrocytes around the cystic cavity after one week. MIF is chemotactic for keratinocytes and facilitates wound healing by macrophages [1]. MIF production by peritoneal macrophages may contribute to paracrine and autocrine activation and to macrophage accumulation in the peritoneal cavity of women with endometriosis [2]. If macrophages in CNS play an important role in its regeneration, MIF depletion could hinder the recovery process after SCI because MIF

mRNA is upregulated in microglia accumulating around the lesion. Astrocytes compose glial scars after SCI to prevent inflammation outflow into circumferential normal tissue. MIF depletion could also negatively affect glial scar formation and functional recovery because MIF is upregulated after SCI in astrocytes [9].

The best way to elucidate MIF function in SCI is to use knockout (KO) mice for a comparison study with wild-type (WT) mice. We injured MIF KO and WT mouse spinal cords using a spinal cord compression apparatus and compared their locomotor recovery for six weeks. We detected a statistically significant difference between KO and WT mice in locomotor scale, immunohistological studies, and in-vitro glutamate assault of cerebellar granular neurons (CGN).

Materials and methods

Animals

In this study, we used female MIF-deficient mice (KO) and wild-type mice (WT), which were established by Honma [8]. Both strains were on a Balb/c background and were bred at Hokkaido University, Japan [13]. All animals were treated and cared for in accordance with the Chiba University School of Medicine Guidelines pertaining to the treatment of experimental animals.

Cell culture

Cerebellar granular neurons (CGN) were prepared from postnatal day-seven WT and KO mice. Fresh cerebella were dissected, and the tissue was dissociated with trypsin (2.5 mg/ml, Invitrogen, Carlsbad, CA, USA) and DNase I (0.3 mg/ml, Roche Applied Science, Indianapolis, IN, USA). Cells were plated on poly-L-lysine-coated chamber slides (Lab-Tek Chamber Slides Permanox, Nalge Nunc International, Rochester, NY, USA) at a density of 7.0×10^4 cells/cm^2 in Dulbecco's modified Eagle medium (DMEM; Gibco BRL, Grand Island, NY, USA), supplemented with 10% fetal bovine serum, penicillin–streptomycin (100 units/ml penicillin G sodium, 100 µg/ml streptomycin sulfate, Invitrogen, Carlsbad, CA, USA), and 0.02 M HEPES. After 16 h in culture, the medium was replaced with DMEM supplemented with penicillin-streptomycin, 20 mM HEPES, N2 supplement (0.01%, Invitrogen), KCl (20 mM), fibronectin (10 µg/ml), and cytosine arabinoside (1.0 µM). Cells were maintained in a humidified atmosphere containing 5% CO_2 at 37°C.

Following seven-day culture, CGN were treated with glutamate (100 µM) for 6 h to induce cell death. Recombinant human MIF (R&D Systems, Minneapolis, MN, USA) was added to the culture medium of glutamate-treated CGN from KO mice in different concentrations (5–50 ng/ml) to assess the effect of MIF on neuronal death. Neuronal death was detected by double staining with propidium iodide and calcein using live/dead double staining kit (MBL, Nagoya, Japan). The numbers of dead cells were counted in two areas of 400× magnification microscope fields and averaged among four groups.

Surgery

Tissue samples were obtained from WT ($n = 24$) and KO ($n = 23$) mice. Under halothane anesthesia, laminectomy was performed at the T7–8 level, leaving the dura intact. The animals were then placed in a stereotaxic apparatus, and two adjustable forceps were applied to the spinous processes of both T6 and T9 to stabilize the spine. The dural tube was compressed with a steady load of 20 g for 5 min at the site of the T 7–8 laminectomy. The tip of the weight was a 1 × 2-mm rectangular plastic plate [5]. The mice were kept under a heating lamp until they regained consciousness. Bladder function was observed during the first few days after trauma for signs of urinary retention. The mice were kept in a temperature-controlled environment of 20°C and were exposed to alternate light and dark periods of 12 h. Food and water were given ad libitum. Manual bladder expression was performed twice a day until recovery of the bladder reflex.

Tissue preparation

Mice were sacrificed 24 h (WT: $n = 7$, KO: $n = 5$), 72 h (WT: $n = 6$, KO: $n = 7$), and 6 weeks (WT: $n = 11$, KO: $n = 11$) after SCI. Animals were perfused transcardially with ice-cold 4% paraformaldehyde in phosphate-buffered saline (PBS) under deep pentobarbital anesthesia. Spinal-cord segments T 6–9 were excised and fixed overnight in the same solution. The tissue was then immersed for 48 h in 20% sucrose in PBS at 4°C, embedded in O.C.T. compound (Tissue-Tek; Sakura Finetech, Tokyo, Japan), and frozen on dry ice. We sliced 12 µm thick cross-sections and mounted every fifth slice on five sequential slides. Each slide had 20 slices. This methodology covered 6-mm spinal cord length around the epicenter of the lesion. The sections were subjected to histological (six weeks after injury), histochemical (72 h), and immunohistochemical (24 h, 72 h, and 42 days after injury) examination.

Histological studies

Immunohistochemistry was performed as previously described [9]. Briefly, the sections were rehydrated in 0.3% Triton X-100 in PBS for 1 h, washed with PBS for 5 min

three times, and blocked with blocking solution (0.05 M Tris–HCl (pH 7.6), 1% bovine serum albumin, Blockace (Yukijirusi, Sapporo, Japan), 0.15 M NaCl, and 0.1% Tween 20) for 1 h. The sections were then incubated overnight at 4°C with mouse antineuronal nuclei antibody (NeuN, 1:400 dilution; Chemicon, Temecula, CA, USA), as a marker for neurons, rabbit anti-caspase-3-active antibody (caspase-3-active, 1:800 dilution; Genzyme Techne, Cambridge, MA, USA), as a marker for apoptotic cells, and adenomatous polyposis coli (APC, 1:800 dilution, CalBiochem, San Diego, CA, USA), as a marker for oligodendrocytes. The slides were then washed with PBS three times for 5 min and incubated with secondary antibodies (goat anti-mouse Alexa Fluor 488 and goat anti-rabbit Alexa Fluor 594, both 1:800 dilution; Molecular Probes, Eugene, OR, USA) for 30 min at room temperature. The slides were then washed with PBS three times and sealed with mounting medium (Dako Cytomation, Copenhagen, Denmark).

Lectin histochemistry was performed using tomato lectin (0.02 mg/ml; Sigma, St Louis, MO, USA) as a marker for microglia, followed by Alexa Fluor 488 streptavidin (1:800 dilution; Molecular Probes). The slides were then washed with PBS three times and mounted as described above.

Cell counts

We counted the NeuN/caspase-3-active or APC/caspase-3-active double-positive cells 24 and 72 h after injury. The double-positive cells indicated the presence of apoptotic cells that were induced by injury. We measured the slices macroscopically, and designated the two smallest slices as the lesion epicenter on each slide of an animal. Slices were selected from the slides and images were captured using a 20× objective lens field. Every cross-section was composed from four images. We printed the images and double-positive cells were counted. Averages were compared between the genotypes. We also counted the tomato-lectin-positive cells and compared these counts between WT and KO mice 72 h after injury as previously described. The positive cells indicated microglia that had gathered in the injured spinal cord.

We counted the cresyl violet-positive neurons in the ventral gray matter whose major diameters were larger than 30 μm as alpha motor neurons [18] and compared these between the WT and KO mice 42 days after injury, as previously described. We also counted surviving oligodendrocytes, which were stained with APC followed by Alexa Fluor 488-conjugated secondary antibody.

Behavioral test

Functional recovery of the hind limb was determined by measuring the hind-limb motor-function score as described previously [6]. Mice were allowed to move freely in an open field with a rough surface for 5 min at each time period tested. The hind-limb movements of mice were videotaped and scored by two independent observers who were unaware of the groups. Measurement of motor function was performed before surgery and 1–6 weeks (once a week) after SCI. The scale ranged from 0 to 13. In brief, a score of 0 indicated complete paralysis, 1–3 indicated movement of hind limbs without rhythmical stepping, 4–5 indicated rhythmical motion of hind limbs without weight-bearing ability, 6–7 indicated weight-bearing ability, 8–12 indicated walking ability with an increase in the hind-limb gait width, and 13 indicated full recovery.

Statistical analysis

Motor-function scores were subjected to repeated-measures ANOVA followed by a post hoc test using the Tukey–Kramer test. The motor-function score of each time point was statistically analyzed using Student's t test. The results of neuronal survival counts 42 days after SCI, apoptotic neuron counts, and tomato-lectin-positive microglia counts after 24 or 72 h were subjected to Mann–Whitney U tests. The numbers of dead cells from glutamate insult in vitro were subjected to one-way ANOVA followed by a post hoc test using the Tukey–Kramer test. Data are presented as mean values ± SE. Values of $p < 0.05$ were considered statistically significant.

Results

MIF deletion attenuated glutamate insult of CGN in vitro

After 6 h of glutamate insult, the number of dead cells was counted and compared between WT and KO (Fig. 1). The number of dead cells in CGN from KO mice (3 ± 0.6 in KO; Fig. 1b, d) was significantly fewer than that from WT (11 ± 1.9 in WT; Fig. 1a, d). We added recombinant human MIF to the culture medium of glutamate-treated CGN from KO mice in different concentrations (5–50 ng/ml) to assess the effect of MIF on neuronal death. Recombinant human MIF exacerbated the effect of glutamate insult on CGN in KO mice, and the number of dead cells was 5 ± 1.7 (5 ng/ml) and 4 ± 1.5 (50 ng/ml) (Fig. 1c, d). These results showed that MIF deletion attenuated the glutamate-induced insult of CGN.

MIF deletion facilitated recovery of hind-limb motor function after spinal cord compression

We assessed recovery of hind-limb function by measuring the hind-limb motor-function score, in which the maximum

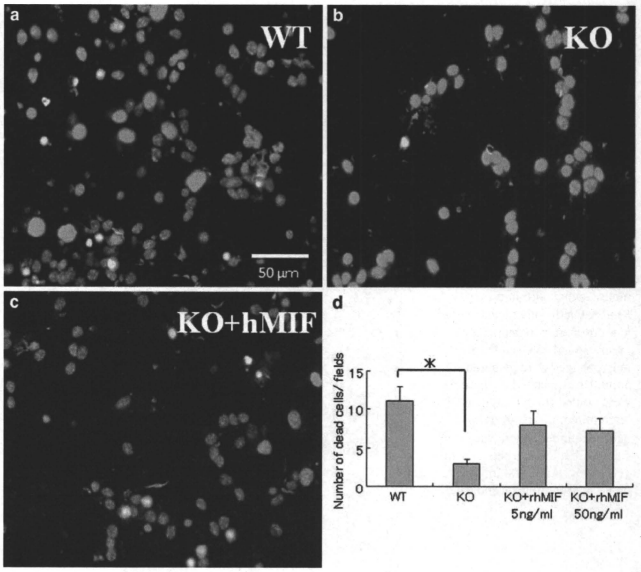

Fig. 1 Cerebellar granular neurons (CGN) from KO mice were more resistant to glutamate insults in vitro. Following 7 days of culture, primary cultured CGN were treated with glutamate (100 μM) for 6 h to induce cell death. Live cells (*green*) and dead cells (*orange*) were stained with live and dead cell staining kit. **a**, **b** More dead cells were stained in CGN from WT mice (**a**) than KO mice (**b**). **c** Recombinant human MIF (5 ng/ml) exacerbated neuron death in CGN from KO mice. **d** Each bar-graph shows the number of dead cells after glutamate insults to CGN from WT, KO, KO + MIF (5 ng/ml), and KO + MIF (50 ng/ml). The number of dead cells in CGN from KO mice was significantly fewer than in CGN from WT mice ($p < 0.05$). Although MIF addition resulted in increased neuronal death in CGN from KO mice, they did not reach a statistically significant difference. *$p < 0.05$. *Bar* 50 μm for **a**–**c**

hind-limb motor-function score was 13. All mice had a score of 11 before SCI, and the score was reduced to 0 immediately after compression. There was no significant difference in motor-function score between the WT and KO mice until three weeks after injury (Fig. 2). Three weeks after compression, significant recovery of hind-limb function was observed in KO mice compared with WT mice

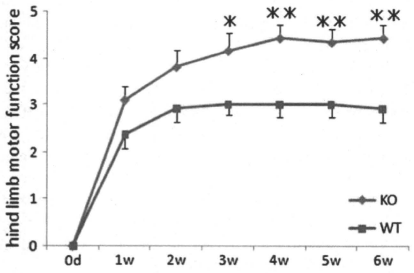

Fig. 2 Hind-limb locomotor score showed better recovery in KO mice after spinal cord compression injury. After spinal cord compression injury, hind-limb locomotor score for each genotype was recorded and compared. The scores of KO mice always surpassed those of WT mice and showed a statistical difference from 21 days after spinal cord injury ($n = 11$ in each genotype). *$p < 0.05$; **$p < 0.01$

(three weeks, $p < 0.05$; four weeks, $p < 0.01$, five weeks, $p < 0.01$; six weeks, $p < 0.001$). The time course of recovery of hind-limb function showed statistically significant differences between the genotypes in repeated-measures ANOVA ($p < 0.01$). The average recovery score in KO mice six weeks after transplantation was 4.45 ± 0.28 (range 2–6), and the corresponding score in WT mice was 2.91 ± 0.28 (range 2–5). A score of 4 indicated a gait characterized by stepping and forward-propulsive movements of one hind limb, but no weight bearing and external rotation of the hind limb. A score of 3.0, however, indicated an obvious movement of one or more joints in both limbs but no coordination, alternate stepping movement, or weight-bearing.

Histochemical assessment shows more neurons survived in KO than WT mice 42 days after SCI

Cresyl-violet-positive cells larger than 30 μm in major axis were classified as remaining motor neurons. Figure 3 shows representative slides of WT (a) and KO (b) spinal cords in the lesion epicenter. In high magnification view, some neurons were spared in the gray matter of the KO mice (d) compared with WT mice (c). Many more inflammatory cells were stained in the gray matter of WT (c) compared with KO (d) mice. The average number of

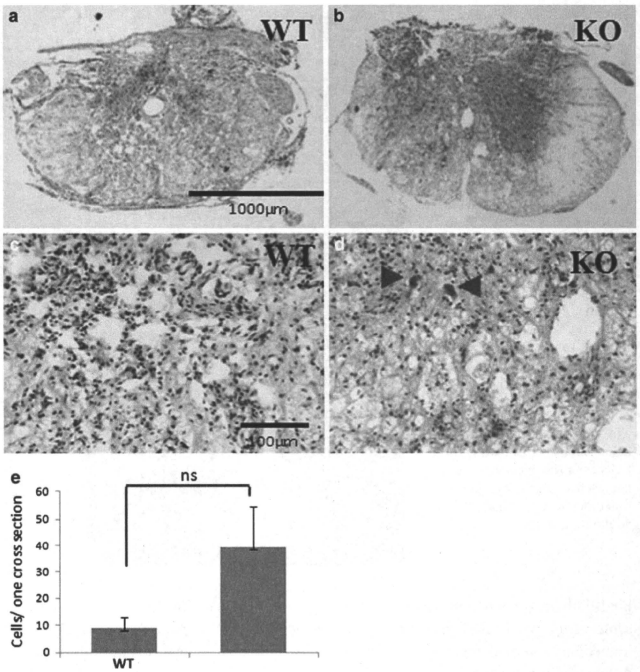

Fig. 3 More neurons survived in KO mouse spinal cord 42 days after spinal cord compression injury. Spinal cord cross-sections, 42 days after spinal cord injury, were stained with cresyl-violet. Motor neurons whose diameter was more than 30 μm were counted and compared. **a**, **b** Representative spinal cord cross-sections of the lesion epicenter 42 days after spinal cord compression injury (**a** = WT, **b** = KO). **c**, **d** High magnification view of **a** and **b**. Some neurons survived in KO mouse spinal cord in **d** (*arrow heads*). On the other hand, a few neurons were counted in WT mouse spinal cord, and more macrophages were gathered around the spaces where neurons were voided (**c**). **e** Despite a large difference in surviving neuron numbers, there was no statistical difference between the genotypes. *Bar* 1,000 μm for **a** and **b**, 100 μm for **c** and **d**

cresyl-violet-positive cells larger than 30 μm in KO mice 42 days after injury was 45.1 ± 15.0, whereas in WT mice it was 12.2 ± 3.9 (Fig. 3e). Although there was no statistically significant difference between genotypes ($p = 0.05$), the number of remaining neurons was indicative of a better recovery of hind-limb motor function in KO mice. On the other hand, there was no statistically significant difference in the number of APC-positive cells between WT and KO mice 42 days after injury (data not shown).

Immunohistochemical assessment a few days after injury showed fewer apoptotic neurons were counted in KO mice; a similar result was obtained for neuron counts after 42 days

As described earlier, more neurons survived in the lesion epicenter of KO mice than in that of WT mice after 42 days, and this result influenced better recovery in hind-limb motor function in KO mice 42 days after SCI. Moreover, more CGNs from KO mice were resistant to glutamate insults than those from WT mice. Based on the above results, we hypothesized that less acute neuronal death occurred in KO mice within a few days after SCI than in WT mice. Thus, we counted NeuN/caspase-3-active double-positive cells and compared between genotypes 24 and 72 h after SCI.

Figure 4 shows fluorescent immunohistochemistry of NeuN (a and b), caspase-3-active (c and d), and merged views (e and f) 24 h after SCI. The number of double-positive cells for NeuN/caspase-3-active in KO mice was significantly smaller than in WT mice 24 and 72 h after injury ($p < 0.05$ after 24 h; $p < 0.01$ after 72 h). The average number of double-positive cells for NeuN/caspase-3-active in KO was 18 ± 3.0 24 h after injury and 15.8 ± 2.1 72 h after injury, whereas that in WT mice was 27 ± 1.9 and 25.2 ± 0.6, respectively (Fig. 4g).

There was no significant difference in the number of microglia 72 h after injury between WT and KO mice ($p = 0.46$). The average number of positive cells for tomato lectin in KO mice 72 h after injury was 372 ± 60, whereas that in WT mice was 436 ± 48.

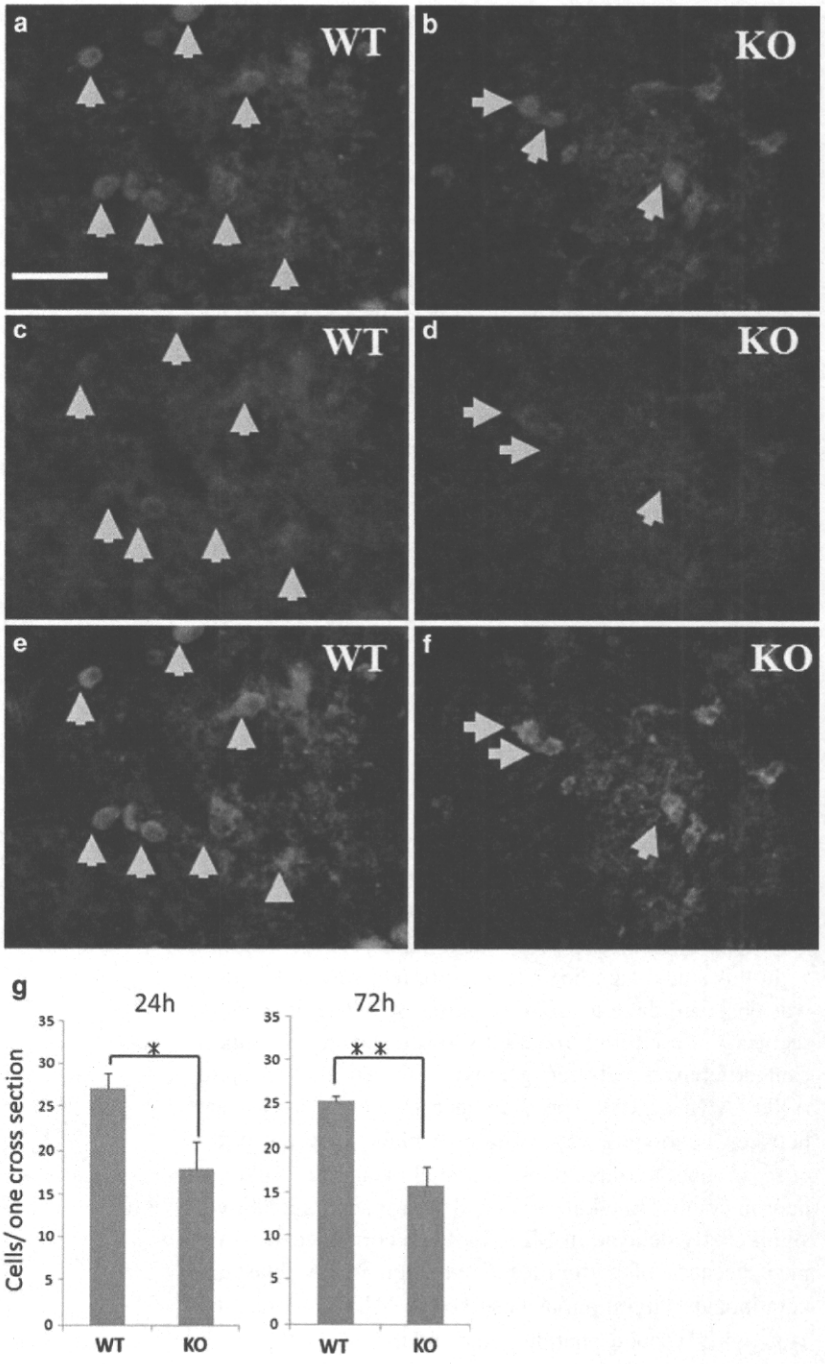

Fig. 4 Fewer NeuN/caspase-3-active double-positive cells were counted in KO mice 24 and 72 h after spinal cord injury (SCI). We counted NeuN/caspase-3-active double-positive cells as apoptotic cells. Double-positive cells were counted and compared between genotypes. **a–f** Representative NeuN/caspase-3-active double fluorescent immunostaining 24 h after SCI. NeuN staining (**a**, **b**), caspase-3-active (**c**, **d**), and merged figures in WT and KO mice (**e**, **f**). Fewer neurons were caspase-3-active in KO mice (*arrow*) than WT mice (*arrow heads*). **g** *Bar graphs* show double-positive cell numbers in WT and KO mice 24 h (*left panel*) and 72 h (*right panel*) after spinal cord compression injury. Significantly fewer double-positive cells were counted in KO mice compared with WT mice 24 and 72 h after SCI. $*p < 0.05$, $**p < 0.01$. *Bar* 50 μm for **a–f**

Discussion

In this study, deletion of MIF suppressed glutamate-induced neuronal death in vitro. Recombinant human MIF exacerbated glutamate-induced neuronal death in CGN from MIF KO mice. In the in-vivo study, MIF KO mice showed a decreased number of apoptotic neurons, better neuronal survival, and better hind-limb functional recovery compared with WT mice after spinal cord compression injury.

Previously, we examined MIF expression in a mouse spinal cord compression injury model [9]. Activated microglia with amoeboid morphology that accumulated in the lesion epicenter expressed MIF mRNA and protein, and the peak of MIF expression was three days after injury. In this study, MIF deletion did not change microglia accumulation in the lesion epicenter three days after SCI. In a lipopolysaccharide-mediated endotoxemia model, MIF released from anterior pituitary glands stimulates macrophages and monocytes to secrete inflammatory cytokines